Retrospective Theses and Dissertations

Iowa State University Capstones, Theses and Dissertations

2006

Automated high throughput protein crystallization screening at nanoliter scale and protein structural study on lactate dehydrogenase

Fenglei Li
Iowa State University

Follow this and additional works at: https://lib.dr.iastate.edu/rtd

Part of the Analytical Chemistry Commons

Automated high throughput protein crystallization screening at nanoliter scale and protein structural study on lactate dehydrogenase

by

Fenglei Li

A dissertation submitted to the graduate faculty

in partial fulfillment of the requirements for the degree of

DOCTOR OF PHILOSOPHY

Major: Analytical Chemistry

Program of Study Committee:
Edward S. Yeung (Major Professor)
Donald C. Beitz
Robert S. Houk
Patricia A. Thiel
L. Keith Woo

Iowa State University

Ames, Iowa

2006

Graduate College

Iowa State University

This is to certify that the doctoral dissertation of

Fenglei Li

has met the dissertation requirements of Iowa State University

Signature was redacted for privacy.

Major Professor

Signature was redacted for privacy.

For the Major Program

To Ella

TABLE OF CONTENTS

ABSTRACT

The purposes of our research were:

1. To develop an economical, easy to use, automated, high throughput system for large scale protein crystallization screening.

2. To develop a new protein crystallization method with high screening efficiency, low protein consumption and complete compatibility with high throughput screening system.

3. To determine the structure of lactate dehydrogenase complexed with NADH by x-ray protein crystallography to study its inherent structural properties.

Firstly, we demonstrated large scale protein crystallization screening can be performed in a high throughput manner with low cost, easy operation. The overall system integrates liquid dispensing, crystallization and detection and serves as a whole solution to protein crystallization screening. The system can dispense protein and multiple different precipitants in nanoliter scale and in parallel. A new detection scheme, native fluorescence, has been developed in this system to form a two-detector system with a visible light detector for detecting protein crystallization screening results. This detection scheme has capability of eliminating common false positives by distinguishing protein crystals from inorganic crystals in a high throughput and non-destructive manner. The entire system from liquid dispensing, crystallization to crystal detection is essentially parallel, high throughput and compatible with automation. The system was successfully demonstrated by lysozyme crystallization screening.

Secondly, we developed a new crystallization method with high screening efficiency, low protein consumption and compatibility with automation and high throughput. In this crystallization method, a gas permeable membrane is employed to achieve the gentle evaporation required by protein crystallization. Protein consumption is significantly reduced to nanoliter scale for each condition and thus permits exploring more conditions in a phase

diagram for given amount of protein. In addition, evaporation rate can be controlled or adjusted in this method during the crystallization process to favor either nucleation or growing processes for optimizing crystallization process. The protein crystals gotten by this method were experimentally proven to possess high x-ray diffraction qualities.

Finally, we crystallized human lactate dehydrogenase 1 (H4) complexed with NADH and determined its structure by x-ray crystallography.

The structure of LDH/NADH displays a significantly different structural feature, compared with LDH/NADH/inhibitor ternary complex structure, that subunits in LDH/NADH complex show open conformation or two conformations on the active site while the subunits in LDH/NADH/inhibitor are all in close conformation.

Multiple LDH/NADH crystals were obtained and used for x-ray diffraction experiments. Difference in subunit conformation was observed among the structures independently solved from multiple individual LDH/NADH crystals.

Structural differences observed among crystals suggest the existence of multiple conformers in solution.

CHAPTER 1 GENERAL INTRODUCTION

DISSERTATION ORGANIZATION

Starting with a general introduction about structural proteomics, x-ray protein crystallography and related techniques, this dissertation continues with three complete scientific manuscripts in the following chapters. A final chapter summarizes the work and provides some prospects for future research.

STRUCTURAL PROTEOMICS

High Throughput Structure Determination

To realize the real value of the wealthy genome sequence information obtained from several completed genome projects, the sequences must be correlated to the proteins they encode and the biological functions of those proteins. Since protein structure determines its function, large scale protein structure determination with the goal of establishing structural function relationships, termed as structural proteomics, has been the natural progression to further characterize the genome in this post-genomic era [1-5].

Protein structure is better conserved than sequence in evolution, comparing protein structures can reveal homology undetectable by sequence comparison and thus can quickly suggest the biological function of an uncharacterized protein [2]. Protein structure and function relationship can also increase understanding of protein design principles and could have application in protein engineering [3]. Protein structure also provides a direct insight into the molecular mechanism of important biological processes [2]. In pharmaceutical industry, protein structure could guide lead molecules optimization process, which has been

proven to be a very challenging task. This strategy of structure-guided or rational drug design has been demonstrated by the success in finding inhibitors for influenza virus neuraminidase and inhibitors for HIV proteinase [4, 9].

X-RAY PROTEIN CRYSTALLOGRAPHY

The current primary methods for three dimensional protein structure determination are x-ray protein crystallography and NMR [5]. Protein structure determination by x-ray crystallography requires a protein crystal in good quality with a reasonable size. NMR is a technique for structure determination from a protein in solution. The difficult protein crystallization process is not required by NMR. However, NMR is normally limited to proteins with molecular weights less than 30K [5]. In contrast, x-ray crystallography can determine protein structure with almost any molecular weight and complexity as long as a well ordered crystal can be obtained. This makes x-ray crystallography the working horse for most protein structure determination nowadays.

History of Protein Crystallography

X-ray crystallography has been an extremely successful technique for small molecule structure determination for more than 70 years [6]. However, protein crystallography is a relative young technique. Although the first published observation of protein crystallization was in 1840 [7], the first protein structure, that of myoglobin, was solved by x-ray crystallography in 1960, only 46 years ago. Since then, protein crystallography has been used for the determination of more than 15,000 protein structures [5, 6].

In the past two decades, protein crystallography was revolutionized by the advances of data collection and computing techniques [6]. The traditional phasing problem of protein crystallography becomes easier because of the emergence of a multiple-wavelength

anomalous diffraction (MAD) technique [8, 14], which benefits from the availability of a tunable x-ray source from synchrotron radiation and the protein expression technique for incorporating seleno-methionine into protein for anomalous scattering [8, 14].

Principles of Protein Crystallography

X-ray is electromagnetic wave in nature. X-ray diffraction by an atom is an interaction between the electrons of the atom and the electric and magnetic components of the x-rays. The electron of an atom oscillates with the same frequency under the influence of the electromagnetic wave of incident x-ray and thus absorbs energy and then emits radiation of the same frequency. The nucleus in the atom can also interact with electromagnetic wave, but it is so massive that its scattering is negligible. There is a relationship between the properties of the emitted radiation (diffracted x-ray light) and the electron density distribution in the atom. For x-ray light diffracted by a molecule, obviously, the properties of the emitted radiation would be decided by the electron density distribution or the structure of the molecule. Therefore, the information on the properties of the diffracted x-ray light can be used to trace back to the electron density distribution in the molecule and thus the molecular structure can be determined [6, 10, 11].

However, the scattered x-ray light by a single molecule is too small to be measured experimentally. If a large number of molecules scatter x-ray light in a cooperatively way so that all the scattered x-ray lights can be summed together in a constructive way (instead of canceling each other), the overall scattered or diffracted x-ray would be much larger than the x-ray light diffracted by a single molecule. If the number of the molecules in cooperation is large enough, the overall scattered x-ray light intensity would be large enough to be detected by a photon sensitive detector such as photographic film or charge coupled device (CCD). For those large numbers of molecules, in order to able to diffract x-ray light in a constructive

way, they have to be well ordered or located periodically in space. Such entity is essentially a crystal [6, 10, 11].

X-ray Sources and Detectors

X-rays are electromagnetic radiation with wavelengths in the range from 1000 angstrom to 0.1 angstrom. For x-ray crystallography, usually x-ray with wavelengths between 1.6 angstrom to 0.5 angstrom are used. In x-ray instrument for general laboratory use, the x-ray light is usually produced by a copper anode at 1.54 angstrom or molybdenum anode at 0.71 angstrom [6, 11].

X-ray generated in this way has limited intensity because of the limited rate of heat dissipation. It is usually difficult to grow large size protein crystals [7]. Therefore, high intensity x-ray light is preferred for protein crystallography. In the past two decades, intense x-ray radiation from electron synchrotrons have become more and more popular in protein crystallography because of its nature of high intensity and tunability in wavelength [10,11].

X-rays with continuous wavelengths make the full range from 0.5 angstrom to 1.6 angstrom fully accessible for use. More importantly, x-rays from synchrotron radiation are wavelength tunable. This makes an important phasing method named as multiple-wavelength anomalous diffraction (MAD) widely used, which makes the traditional phasing problem becomes much easier to solve [14].

Single Photon Counters were used in the early days of x-ray crystallography, providing very accurate measurement. However, it takes a long time (weeks) to finish one complete data set because of its sequential nature.

Photographic film had been a classic detector for crystallography. It is an area detector. Though less sensitive, photographic film has superior resolution to modern area detectors.

Image plates as x-ray detectors have the advantage of one magnitude higher sensitivity and much larger dynamic range over photographic film. In addition, it is more sensitive at short wavelengths that make absorption correction unnecessary [10].

Charge coupled devices (CCD) have been used as the detectors. It is more sensitive than photographic film. It has large dynamic range, excellent spatial resolution, low noise level and fast data transfer rates [10].

Solving Structures

The mathematical principles behind x-ray diffraction are not complicated. The diffraction pattern formed by a crystal is the Fourier transform of the crystal. However, in the x-ray diffraction experiments, only intensities of those diffracted x-rays are recorded on detectors. The phase information, which is critical for description of the diffracted x-ray is totally lost. It's not a real problem for small molecules because of the limited number of atoms involved in diffraction and thus limited possibilities of phases. However, for protein crystallography, the number of atoms in a protein molecule is very large and thus makes the phasing problem difficult to solve.

Taking advantage of other information available, for protein crystallography, the following methods have been mainly used for solving the phase problem: Molecular Replacement, Isomorphous Replacement and Anomalous Scattering,

Molecular Replacement

If a similar protein structure is available, the structure of the unknown protein molecule can be solved by the method named molecular replacement solely from the intensities of diffraction pattern without any experimental or other phase information. This method has been getting more and more application with more protein structures determined resulting from the efforts of structural proteomics.

Isomorphous Replacement

Based on the fact that more than 50% content of a protein crystal is solvent, M. F. Perutz [12, 13] developed a phasing method called Isomorphous Replacement. In this method, heavy atoms can be introduced into protein crystals by diffusion to generate crystal derivatives, which are structurally identical to the native crystal with the only exception of the presence of the heavy atoms. Since heavy atoms scatter x-ray light more strongly than light ones because of their higher atomic number, diffraction data from a series of crystal derivatives contain useful phase information sufficient for solving the structure of the native crystal.

Anomalous Scattering

There are two ways to use anomalous dispersion for phase determination: single-wavelength anomalous dispersion (SAD) and multiple-wavelength dispersion (MAD). With the advent of powerful synchrotron radiation and protein expression technique, multiple wavelength anomalous scattering has almost become the standard method for phase determination.

To use anomalous dispersion, anomalously scattering atoms are incorporated into recombinant proteins by replacing normal sulfur-containing methionine with selenium methionine. The selenium atoms normally sufficiently provide anomalous scattering in a crystal. For SAD, two data sets are collected on both native and derivative crystals. Only one wavelength is chosen. In a similar way to Isomorphous Replacement, phase information can be obtained. For MAD, since anomalous scattering power of selenium atoms is radiation wavelength dependent, a series of diffraction patterns with appreciable changes in intensity can be generated by simply varying the wavelength of incident x-ray synchrotron radiation [14]. Phase information can be obtained by solely using the anomalous dispersion as in MAD method. In a MAD structure determination, since only one crystal is used for the entire data

collection, isomorphism is perfect. Moreover, unlike isomorphous replacement, MAD can provide good phase information at high resolution [6, 14].

PROTEIN CRYSTALLIZATION

Characteristics of Protein Crystals

There are significant differences between protein crystals and small molecule (inorganic or organic) crystals in many aspects including physical (such as optical properties) and mechanical properties, growth mechanism and internal networks forming crystal lattice. Those differences have profound implications on protein growth methods, x-ray diffraction data collection strategies and data qualities [15-24].

The striking and important difference between protein crystals and small molecule crystals is the high percentage of solvent in protein crystals, which is normally 50% to 70% [25]. This feature of protein crystals results in their unique diffraction and other physical properties. Protein crystals are thus mechanically very weak. Great care needs to be taken for protein crystal handling. Protein molecules in a crystal are surrounded by ordered, structural water molecules, which make the protein molecules still biologically active [27], and thus very likely have similar structures as in solution.

Resulting from the large amount of solvent content, for storage or data collection, protein crystals must be preserved in an environment with humidity control or must be flash cooled at cryogenic temperature for keeping hydration and thus integrity. Otherwise, protein crystals will lose water and completely lose internal order and their diffraction capabilities. [28-34]

There are fewer and weaker lattice constraints in a protein crystal than small molecule crystals. The interactions among protein molecules are also weak. Therefore, protein crystals

are generally less ordered and show lower diffraction qualities compared with traditional crystals [15-34].

Principles of Protein Crystallization

Some studies show protein growth mechanisms are similar to those for small molecule crystals, which include spiral dislocations, two-dimensional nucleation on surfaces, random nucleation and normal growth [19, 21, 35].

It has been shown by AFM study that the characteristic kinetic parameters of protein crystal growth are significantly lower than those for traditional crystals by a factor of two or three magnitudes [15, 17, 36-41]. In practice, small molecule crystals can grow in minutes or days while protein crystallization takes days to weeks or even months.

Protein crystallization normally occurs at conditions at which protein molecules are in their native conformations. These conditions are normally neutral, biological pHs, biological temperatures and non-denaturing conditions.

METHODS FOR PROTEIN CRYSTALLIZATION

There are currently two main methods for protein crystallization: Vapor diffusion and microbatch. The main goal of these two crystallization methods is to achieve supersaturation at a slow rate since proteins take long time to crystallize (If the supersaturation is achieved too fast, precipitation instead of crystals will be obtained.).

Vapor Diffusion

There are two modes of this method: sitting-drop and hanging-drop. Usually two microliter protein solution is mixed with two microliter precipitant/well solution and then is dispensed to a siliconized cover slip. For hanging drop method, the mixed protein/precipitant solution drop is suspended by surface tension on the surface of an inverted cover slip, which

forms a close chamber by covering and sealing a well with precipitant solution inside. For sitting-drop method, the mixed protein/precipitant solution drop sitting on the bottom of a well is physically separated in solution phase from the precipitant solution by a barrier in the well, but it is connected in the air phase with the precipitant solution. Resulting from the difference in the concentration of precipitant, there is a vapor diffusion process occurring between two solutions in vapor diffusion methods. Since it is a slow vaporization process, it greatly favors the slow protein crystallization process.

Vapor diffusion is a popular method for protein crystallization, especially for manual operation of the experiments. It is suitable for screening a large range. Moreover, it is economic, convenient and easy to perform manually.

Microbatch

To use this method, microliter protein solution is mixed with precipitant solution and then put in an oil drop. A series of precipitant concentrations will be used for screening purpose. But, for one drop, the concentration of the precipitant usually does not change much over the time. Basically only one condition is explored for each drop in the oil. The advantage of this method is that the best crystallization can be well defined in the screening experiments since the condition for each well is not changed over time. This is good for later optimization experiment to grow larger crystals.

HIGH THROUGHPUT SCREENING FOR PROTEIN CRYSTALLIZATION

Despite the great efforts on studying protein crystallization mechanisms [15, 17, 19, 21, 35-41], protein crystallization is still currently underdeveloped science, which is mainly a trial-and-error procedure [10].

Currently, there is still no effective theories that can help predict protein crystallization conditions. Therefore, the practical strategy is to screen a large number of combinations of pH, salt concentration, precipitants and so forth. If any promising conditions are found, further finer screening will be executed with the goal of optimizing the condition for growing large size crystal for x-ray diffraction experiments.

Problems of Current Methods

The traditional crystallization methods such as vapor diffusion and microbatch method are currently employed for large scale crystallization screening. The mechanical operations required for applying these two methods are relatively complicated for automation. Therefore, in most efforts on achieving high throughput and automated crystallization screening, various robots are employed [42-49].

Although the strategy of employing robots has achieved impressively high throughput, robots are expensive and demand professional maintenance from time to time and are not accessible for most biologists and regular users. The visible light detection method in those systems often encounters the difficulty of complicated background. In addition, for microbatch method, the crystallization components in the mother liquor sometimes can interact with oil and interfere with the crystallization process [50].

THE GOALS

The first goal is to develop an economical, easy to operate, high throughput and automated system without using high cost high maintenance robots. The second goal is also to develop a new crystallization method that can provide high screening efficiency, low protein consumption, complete compatibility with automated, high throughput screening systems. The third goal is to develop a new detection scheme that can eliminate the common false positives but still work in a high throughput automated manner.

At last, the fourth goal is also to use protein crystallography tools to determine the structure of LDH/NADH complex in order to reveal the inherent structural properties of this important enzyme.

REFERENCES

(1)   Yee, A.; Paradee, K.; Christendat, D.; Savchenko, A.; Edwards, A.; Arrowsmith, C. Acc. *Chem. Res.*, **2003**, 36, 183

(2)   Steven, E. *Nature Reviews,* **2001**, 2, 801

(3)   Skolnick, J.; Fetrow, J.; Kolinski, A.; *Nature Biotechnolog,y* **2000**, 18, 283

(4)   Schmid, M.; *Nature Reviews, Microbiology*, **2004**, 2, 739

(5)   Blundell, T.; Jhoti, H.; Abell, C.; *Nature Reviews,* **2002**, 11, 45

(6)   McPherson, A., Introduction to macromolecular crystallography, 2003, Wiley-Liss, Inc.

(7)   McPherson, A., Crystallization of biological macromolecules, cold spring harbor laboratory press, 1999

(8)   Ealick, S. Curr. Opin. Chem. Biol. 2000, 4, 495

(9)   Greeer, J., Erickson, J., Baldwin, J., Warney, M. J. Med. Chem., 1994, 37, 1035

(10)   Drenth, J. Principles of protein x-ray crystallography, 2nd edition, Spinger-Verlag New York Inc. 1999

(11)   Blow, D. Outlines of crystallography for biologists, Oxford University Press, 2002

(12)   Boyes-Watson, J., Davidson, E. and Perutz, M., 1947, Proc. Roy Soc. (London) Ser. A. 191, 83

(13)   Bragg, W. and Perutz, M. 1954 Proc. Roy. Soc. A225, 315

(14)   Hendrickson, W., Smith, J. and Sheriff, S., Method in Enzymology, 1985, 115, 90, Academic Press, N.Y.

(15) Malkin, A., Land, T., Kuznetsov, Y., DeYoreo, J. and McPherson, A. 1995, Nat. Struct. Biol. 2 956

(16) McPherson, A., Malkin, A., and Kuznetsov, Y. 1995, Structure, 1995, 3, 759

(17) Malkin, A., Kuznetzov, Y., Glantz W., and McPherson A., 1996, J. Phys. Chem., 100, 11736

(18) Rosenberger, F., J. Cryst. Growth, 1986, 76, 618

(19) Biostelle, R. and Astier, J., 1988, J. Cryst. Growth 1988 90 14

(20) Rosenberger, F., Vekilov, P., Muschol, M. and Thomas, B. J. Cryst. Growth 1996, 168, 1

(21) Feigelson, R. J. Cryst. Growth 1988, 90, 1

(22) Durbin S., Annu. Rev. Phys. Chem. 1996, 47, 171

(23) Chernov, A., and Komatsu, H., Science and technology of crystal growth,(ed. J. P. can der Eerden and O.S.L. Bruinsma) 1995, 96, Kluwer, Dordrecht, the Netherlands

(24) Ealick, S. Curr. Opin. Chem. Biol. 2000, 4, 495

(25) Mathews B. 1968, J. Mol. Biol., 1968, 33, 491

(26) Bernal, J. and Crowfoot D., Nature, 1934, 794

(27) Mozzarelli, A. and Rossi, G., Annu. Rev. Biophys. Biomol. Struct. 1996, 25, 343

(28) Blundel, T. and Johnson, L. Protein crystallography, 1976, Academic Press, New York

(29) King, M., Acta Crystallogr., 1954, 7, 601

(30) Hass, D., Biophys. J. 1968, 8, 549

(31) Hope H., Acta Crystallogr. B 1988, 44, 22

(32) Hope H., Annu. Rev. Biophys Biophys. Chem., 1990, 19, 107

(33) Kottke, R. and Stalke D., J. Appl. Crystallogr. 1994, 26, 615

(34) Garman, E., and Schneider, R., J. Appl. Crystallogr. 1997, 30, 211

(35) Mulin, J., Crystallization 3rd ed., Butterworth-Heinemann, Oxford, United Kingdom 1993

(36) Buckley, H. Crystal growth, Crystal growth, Wiley, London 1951

(37) Chernov, A. Modern crystallography vol. III, Crystal growth, Springer-Verlag, Berlin, 1984

(38) Kuznetsov, Y., Malkin, A., Greenwood, A. and McPherson, A., J. Struct. Bil., 1995, 114, 184

(39) Malkin, A., Land, T., Kuznetsov, Y., McPherson, A. and DeYoreo J. 1995 Phys. Rev. Lett. 1995, 75, 2778

(40) Kuznetsov, Y., J. Cryst. Growth., 1996, 166, 913

(41) Malkin, A., Kuznetsov Y. G., and McPherson, A. J. Struct. Biol. 1996, 117, 124

(42) Luft, J., Collins, R., Fehrman, N., Lauricella, A., Veath, C. and DeTitta, G. Journal of Structural Biology 2003 142 170

(43) DeLucas, L. J., Bray, T. L., Nagy, L., McCombs, D., Chernov, N., Hamrick, D., Cosenza, L., Belgovskiy, Stoops, B. and Chait, A. Journal of Structural Biology, 2003, 142, 188

(44) Hosfield, D., Palan, J., Hilgers, M., Scheibe, D., McRee, D. E. and Stevens, R. C. 2003, 142, 207

(45) Watanabe, N., Murai, H. and Tanaka, I. Acta Cryst. 2002, D58, 1527

(46) Walter, T. S., Diprose, J., Pickford, M., Owens, R. J., Stuart, D. I. and Harlos, K. J. Appl. Crystgr. 2003, 36, 308

(47) Rupp, R. Acc. Chem Res. 2003, 36, 173

(48) Heinemann, U., Bussow, K., Mueller, U. and Umbach, P. Acc. Chem. Res. 2003, 36, 157

(49) Luft, J. R., Wolfley, J., Jurisica, I., Glasgow, J., Fortier, S. and DeTitta, G. T. J Cryst. Growth 2001, 232, 591

(50)   Chayen, N. E. Acta Cryst. 1998, D54, 8

CHAPTER 2 AUTOMATED HIGH THROUGHPUT NANO LITER SCALE PROTEIN CRYSTALLIZATION SCREENING

Fenglei Li and Edward S. Yeung*

ABSTRACT

A highly efficient method has been developed for automated and high throughput nanoliter scale protein crystallization screening. The overall system consists of liquid dispensing, crystallization and detection and serves as a whole solution to protein crystallization screening. The novel, cost-effective, high throughput, automated liquid dispensing system can dispense protein and multiple different precipitants in nanoliter scale and in parallel. A new detection scheme, native fluorescence, with a joint complementary visible light detection, has been employed in this system for detecting the protein crystallization screening results. The detection part has the capability of distinguishing protein crystals from inorganic crystals in a high throughput and non-destructive way. The whole method from liquid dispensing, crystallization, to crystal detection is essentially parallel, high throughput and automatic. The system was successfully demonstrated by lysozyme crystallization screening.

INTRODUCTION

In the past few years, an incredible wealth of genetic sequence information enabling our better understanding on many living organisms has become available with the completion of several genome projects [1-3]. These genetic information must be correlated to the biological functions of the proteins they encode for realization of their real values [2]. The biochemical functions of proteins, the working agents of life, are decided by their three dimensional structures [2]. Therefore, functional genomics or proteomics including the determination of three dimensional structures of protein has been considered the natural but critical next step after genome sequencing era [2].

Structural proteomics is an effort to determine the three dimensional structures of proteins on a genome-wide scale in order to facilitate a better understanding of the relationship between protein sequence, structure and function [2]. Several pilot structural proteomics, aiming to generate a set of experimentally determined and computationally augmented protein structures representing most tractable proteins, have been underway [1, 2, 4, 9].

There are two primary techniques at present available for three dimensional protein structure determination at atomic resolution—x-ray crystallography and nuclear magnetic resonance (NMR) [11]. X-ray crystallography can be used to determine the structures of those proteins crystallizable, which is the case for most globular proteins, regardless of protein size and complexity [11]. NMR can be employed to determine the structures of proteins in solution, which don't have to be crystallized. It has the advantage of defining some certain dynamic properties of proteins. But NMR is generally limited to proteins with molecular weight of less than 30 kDa [11].

Currently, the predominant method for determination of three dimensional structures of biological macromolecules is X-ray crystallography [12]. Significant advances have been

achieved in protein preparation, X-ray data analysis and so on [13]. However, protein crystallization still remains as a bottleneck of X-ray crystallography [13]. Protein crystallization is currently still a "black area" with trail-and-error processes. There is no theory or recipe that can effectively predict the conditions where a protein crystallizes [15]. The current method to get around this problem is to screen a large number of chemical and physical conditions such as pH, temperature, ionic strength and concentrations of precipitant and additives [14, 15] to determine the initial crystallization conditions. Obviously the number of conditions that need to be screened will be quickly added up at an exponential rate. This requires a large amount of protein. However, even though one employs the most recent methods for cloning and protein expression, only submilligram or lowmilligram proteins can be generated without stupendous expenditures of resources [19]. The conventional crystallization methods usually use microliter protein sample for each condition they screen. The availability of protein essentially limits the number of conditions that can be screened. The traditional methods such as vapor diffusion and microbatch method are also labor-intensive and time-consuming. Developing high throughput, automatic and miniaturized protein crystallization method is critical if one also considers the fact that there are about 20,000–25,000 protein-coding genes in human genome [22].

There are some efforts on improving the throughput of protein crystallization screening and decreasing protein consumption in recent years [15-19]. However, most of them were involved in using sophisticated and expensive commercial liquid handling system in order to be able to deliver nanoliter solutions in a high throughput. These work employed the regular or modified vapor diffusion method or microbatch method, which usually requires sophisticated operations by expensive robots for automation. The visible light detection scheme employed in those work suffers the problems such as complicated background which makes crystal reorganization more difficult and incapability of distinguishing protein crystals from inorganic crystals. In those works, each well was

detected in a sequential way and thus the throughput is limited. In the current work, a novel, inexpensive and easy-made liquid handling system was introduced. This system has the capability to deliver multiple nanoliter protein solutions and precipitants simultaneously and thus significantly improves the throughput of protein crystallization screening. A brand new protein crystallization we just developed [20] is employed in this system. It is highly amenable to automation and high throughput and essentially eliminates the need for complicated robots. Moreover, here we introduce a brand new detection scheme, fluorescence detection, to protein crystallization screening research field. This detection scheme provides a novel capability of distinguishing protein crystals from inorganic crystals, which can't be done by the regular visible light detection scheme. The fluorescence detection designed in this system is especially highly compatible with automatic and high throughput protein crystallization screening. Working with a complementary visible light detection scheme in the same system, fluorescence detection provides a new but better solution for protein crystallization screening detection compared with the regular detection method. Each step in this system is especially suitable for automation and high throughput. The overall system provides a much better solution to every step required in protein crystallizations screening process: liquid handling, crystallization and detection.

EXPERIMENTAL SECTION

Parallel Liquid Handling System

The liquid handling system consists of one syringe pump, two 81-capillary bundles and 81 vials containing different precipitants (Table 1). Each vial is full of one kind of precipitant and has one capillary as inlet and one as outlet. Each vial is sealed by a cap. All inlet capillaries are connected to the syringe pump via PEEK tubing. All outlet capillaries are

fixed at a capillary array holder and carefully aligned so that all the openings are in the same plane. The syringe pump was controlled by a personal computer. A 5mL syringe was used on the syringe pump. The syringe pump was purchased from Kloehn Ltd, Las Vegas, NV. The capillaries were purchased from Polymicro (Polymicro Technologies, LLC, Phoenix, AZ), whose inner diameter is 250 micrometer and the outer diameter is 360 micrometer. PEEK tubing was purchased from Upchurch Scientific, Inc. (Oak Harbor, WA). The small CCD and the three dimensional translational stage was purchased from Edmund Optics.

Before every use of this system, care was taken to make sure the syringe was full of water and free of air bubbles; all the inlet capillaries between the syringe and the vials were full of water and free of air bubbles as well; the vials were carefully filled with all kinds of precipitants desired for screening and free of air bubbles; each outlet capillary was filled with the precipitant which it is connected to and free of air bubble.

81-well Protein Crystallization Plate

The protein crystallization plate is made of fused silica. The plate was made by ultrasonic machining because of the brittle property of fused silica. It has 9 by 9, totally 81, small wells. The diameter of each well is 1.2 mm and the spacing between wells is 500 nm. The depth of each well is 2.5 mm. The fused silica was purchased from Heraeus Optics, Inc. Before each use, the plate was carefully cleaned by an ultrasonic device.

Fluorescence Detection System

The detection system is showed as Figure 4. The excitation source is a 500 W Hg(Xe) Arc lamp(Oriel, Stamford, CT). An intense UV band (270-320 nm) comes from the lamp. Three optical filters were employed as excitation filters. These three filters are as follows: a color glass filter (UG-5, Schott Glass, Duryea, PA; 80% transmittance between 250-380 nm;

85% transmittance at 280 nm); a customized interference band-pass filter(Omega Filters, Brattleboro, VT; center wavelength: 280 nm, 20% transmittance; FWHM: 35 nm); an interference band-pass filter (CVI, Albuquerque, NM; FWHM: 10 nm; center wavelength: 280.0 nm.). The UV mirror (CVI, Albuquerque, NM) reflects 99% of the light between 250 and 290 nm. A long-pass color glass filter (WG320, Melles Griot, Irvine, CA) and an Interference Filter (center: 350 nm, FWHM: 10 nm) serve as emission filters to block the scattering light. The native fluorescence from protein crystals is collected by a Nikon quartz camera lens (Nikon, f: 4.5, f.l.: 105 mm). A 16-bit, back-illuminated CCD camera (TE/CCD-512-TKB, Princeton, NJ) is employed for the imagining. The CCD has about 40% quantum efficiency in UV region.

Visible Light Detection System

The visible light detection system is in the same system as shown in Figure 2.

When visible light detection scheme is used, the UV light is blocked and vice versa.

The light source for visible light detection is regular fluorescent luminaire. In the visible light detection mode, the emission filters used in fluorescence detection mode serve as neutral density filters. The same camera lens and CCD camera are used for imagining.

Materials and Reagents

Sodium phosphate was purchased from Fisher Scientific. TrisHCl (Tris(hydroxyl)aminomethane hydrochloride), sodium hydroxide, hydrochloric acid, sodium acetate, sodium chloride, HEPES (4-(2-hydroxyethyl)piperazine-1-ethanesulfonic acid sodium salt) were purchased from Hampton Research, Inc. CHES(N-cyclohexyl-2-aminoethanesulfonic acid), sodium citrate CAPS(N-cyclohexyl-3-aminopropanesulfonic acid), were purchased from Sigma. Lysozyme was purchased from Seikagaku Corporation.

All buffers were freshly prepared by adding appropriate aliquots of concentrated components purchased from Hampton Research Inc., Fisher Scientific and Sigma. The pHs were adjusted by adding appropriate amount of 1M sodium hydroxide or 1M hydrochloric acid solution purchased from Hampton Research Inc and were confirmed by a calibrated pH meter.

Lysozyme solutions were prepared by dissolving powders in the appropriate buffer and then centrifuged to get rid of any solid substances.

RESULTS AND DISCUSSION

Parallel Liquid Aspiration and Dispensing

The system is shown in Figure 1. Each vial containing one certain precipitant is sealed by a cap and thus a closed system with one inlet capillary and one outlet capillary forms. Care was taken to ensure that the capillaries and vials were free of air bubbles. Therefore, for each vial, the same amount of solution is pushed into the outlet capillary if there are some solution pushed into the vial from the inlet capillary since liquid is not compressible and the vial is sealed by the cap. The syringe pump is controlled by a personal computer. The total motion of the stepping motor in the syringe pump can be divided into 48,000 steps. Therefore, each step of the stepping motor is responsible for about 0.104 uL (5000 uL is divided by 48000) solution dispensed to or aspirated from 81 capillaries. For each step of the stepping motor and each capillary, about 1.3 nL solution is aspirated from or dispensed into. Since the length, the inner diameter and inner surface friction are the almost same for all 81 capillaries, the volume of the solution aspirated or dispensed is the almost same for each individual capillary for each step of the motor (provided that the viscosity for the solution in each capillary is very similar; if not, the capillary bundle can be easily

designed to be heated up to lower the viscosity to make all solutions have similar viscosities). There is minute dilution because of the introduction of water from the syringe to each vial. The volume of each vial is about 1.8 mL, so the dilution factor is 1.33% if 24 uL is introduced to each vial. Practically, this system can simultaneously aspirate or dispense 81 different solutions from 20 nL to 24 uL. The maximum volume is decided by the total length of the capillary and the tolerance of the dilution factor (for example, for 1.33% dilution factor and 50 cm capillary length, the maximum volume for each precipitant the system can handle is 24 uL.).

Figure 2 shows the system dispenses 100nL and 200nL solutions in parallel. A six-way valve is employed on the syringe pump. One way is for aspirating water into the 5mL syringe. One way is for waste. One way is for connection to capillary bundle. The rest ways are not used. The system can aspirate water from an inlet water bottle and then dispense water into capillaries by switching between ways of the 6-way valve. The precipitant solutions in the 81 vials are replaced after certain time to avoid the excess dilution.

The precipitants in vials are shown in Table 1.

There is no fundamental reason that the system has to be limited to 81 wells. It could be further scaled up if larger syringe and more powerful syringe pumps are employed, which is usually not a problem at all.

Crystallization

A fused silica crystallization plate with 81 micro wells as described in the experimental section was employed for the protein crystallization screening experiments. Figure 3 shows the crystallization plate and its comparison with a traditional VDX 24-well crystallization plate and a penny coin. A 50mg/mL lysozyme solution is used for the demonstration. The liquid handling system described earlier was used to aspirate solutions

from sample reservoirs into each capillary in the capillary bundle and to dispense solutions from each capillary to the target micro well in the crystallization plate.

Firstly, the outlet capillaries were fully filled with precipitants and then 100 nL water from a water reservoir was aspirated into each outlet capillary in the bundle. The 100 nL water plug in each capillary serves as an isolation layer between protein solution and the precipitant in each capillary to avoid the possible precipitation because of their direct contact. Second, the water reservoir was replaced with a lysozyme solution reservoir and 100 nL lysozyme solution is aspirated into each capillary. Third, the lysozyme solution reservoir was replaced with the 81-well crystallization plate. The alignment between the capillary array head and the crystallization plate was done by manual adjustment of the three dimensional translational stage, assisted by a small CCD camera and one TV monitor. After the alignment was done, 100 nL lysozyme solution was dispensed to each micro well on the crystallization plate. Fourth, 200 nL solution from each capillary was dispensed into a waste reservoir. Fifth, the waste reservoir was replaced by the crystallization plate again and 100 nL precipitant solution from each capillary was dispensed into each micro well on the crystallization plate.

After liquid dispensing, there are 100 nL lysozyme solution and 100 nL certain precipitant in each micro well. The crystallization process was done by a new crystallization method described in our paper [19].

The time that crystallization process takes depends on the protein and precipitants used and other experimental factors such as temperature, pH, etc. For the system demonstrated here, it usually takes about three or four hours, which is usually faster than the traditional vapor diffusion method and microbatch method.

Fluorescence Detection System

For the detection of protein crystallization screening, visible light microscopy is widely used [15-20]. In protein crystallization screening, people usually need to make a decision whether a crystal showing up is a protein crystal or an inorganic crystal coming from buffer or precipitant in order to know which direction the further screening should go. Currently, there are three methods available to know the answer. One is to mount the crystal in question on the X-ray instrument to take a look at the diffraction pattern. But this method is not amenable for high throughput or automation. Moreover, most of time crystals showing up in the screening experiments are small and may not be able to diffract light well on home X-ray instrument, which is usually the accessible resource for x-ray diffraction experiments. Another method is to use mechanical force to press the crystal to do so called "crush test". If one hears the sound of click or see the suspect crystal becomes several smaller crystals, then it's an inorganic crystal. If one sees the crystal becomes powder and does not hear anything, that means he just crushed "a perfect good protein crystal". Protein crystals are generally extremely expensive and very hard to crystallize. Therefore, developing non-destructive methods is highly desired. One commercial company markets one small molecule dye which can fill the solvent channels in protein crystals to make the protein crystals look blue. The dye won not give the inorganic salts a blue color because inorganic crystals do not have solvent channels inside [20] and thus the small molecule dye won not be able to get inside the inorganic crystals. This method is non-destructive, but it is not amenable to automation and high throughput. It is highly desired to develop a detection scheme which is not only non-destructive but also amenable to high throughput and automatic protein crystallization screening detection. Here we introduce the fluorescence detection to high throughput and automated protein crystallography research field. Complementarily working with the transmitted visible light detection method in the system, fluorescence detection mode allows instantly distinguishing protein crystals from inorganic crystals without any complicated

experimental operation, which all other traditional and current methods can not do, according to our knowledge, and thus enables high throughput and automatic detection of protein crystals in the crystallization screening processes.

Figure 6 shows the comparison of the fluorescence image and the visible light images for the same set of crystals including one inorganic crystal, which is sodium chloride as an example here. All protein crystals show up in both fluorescence and visible light fluorescence images, but the inorganic crystal only shows up in the visible light image. By careful optical design, most of the Raleigh scattering lights from crystals (no matter from protein crystals or inorganic crystals) were not collected by the camera lens. There are three critical factors here: the excitation filter, the emission filter and the angle between the excitation beam and the crystallization plate. One color glass filter, one band-pass interference filter (FWHM: 35 nm) and one narrow band interference filter (FWHM: 10 nm) are combined together to serve as the excitation filters so that only very narrow band light around 280 nm can pass through to reach the crystallization plate. Two optical filters worked together to only allow a narrow band of lights around 350 nm to pass through to reach the CCD camera. A angle of 30 (roughly) between the excitation beam and the crystallization plate was chosen to reduce most of the scattering lights. The rest of the scattering lights are ignorable or can be easily distinguished from fluorescence by setting up a right cutoff threshold when images are processed.

Visible Light Detection System

There is also a visible light detection mode in this system since it can give different information than the fluorescence mode. Two complementary detection modes working together in the same system enables a better detection for protein crystallization screening, especially suitable for high throughput and automatic screening. The image of protein

crystals taken by the system in the visible light detection mode is shown in Figure 7. the quality of the image can be improved by improving the quality of camera lens, choosing the right intensity of visible light and the right neutral density filters. Any questionable images of subjects can be examined or even possibly identified by comparing both fluorescent image and the visible light image.

CONCLUSION

A novel high throughput system for protein crystallization screening was developed. The liquid handling subsystem is able to aspirate or dispense 81 different or the same solutions in a high throughput and parallel way. The minimum volume of the solutions the system can handle is up to 20 nL and the maximum is up to 24 uL. Employing small amount of protein as of nanoliter significantly reduces amount of the protein required and thus significantly increases the number of the conditions that can be screened. It also significantly reduces the time and efforts the cloning and protein expression require and thus speeds up the whole process of structure determination. A brand new detection method, fluorescence detection method, which is highly compatible with high throughput and automatic protein crystallization screening, was introduced. The two detection schemes working complementarily, the fluorescence and visible light methods, provide the system with the novel capability of distinguishing protein crystals from inorganic crystals in an automatic, non-destructive and high throughput way, which no other method can do. The whole system is cost effective. Each subsystem is especially designed and highly suitable for high throughput and automation. The crystallization of lysozyme was successfully demonstrated on this system.

ACKNOWLEDGEMENT

REFERENCES

(1)   Steven E. B. *Nature Reviews,* **2001**, 2, 801

(2)   Yee A.; Paradee K.; Christendat, D.; Savchenko, A.; Edwards, A. M.; Arrowsmith, C. H. Acc. *Chem. Res.,* **2003**, 36, 183

(3)   Skolnick, J.; Fetrow, J. S.; *TIBTECH,* **2000**, 18, 34

(4)   Skolnick, J. ; Fetrow, J. S.; Kolinski, A.; *Nature Biotechnolog,y* **2000**, 18, 283

(5)   Jhoti, H.; *Trends in Biotechnology,* **2001**, 19, S67

(6)   Burley, S. K.; Bonanno, J. B.; *Current Opinion in Structural Biology,* **2002**, 12, 383

(7)   Teichmann, S. A.; Murzin, A. G.; Chothia, C.; *Current Opinion in Structural Biology,* **2001**, 11, 354

(8)   Stevens, R. C., Yokoyama, S.; Wilson, I. A.; *Science,* **2001**, 294, 89

(9)   Schmid, M. B.; *Nature Reviews, Microbiology,* **2004**, 2, 739

(10)   Blundell, T. L.; Jhoti, H.; Abell, C.; *Nature Reviews,* **2002**, 11, 45

(11)   Bray, T. L.; Kim, L. J.; Askew, R. P.; Harrington, M. D.; Rosenblum, W. M.; Wilson, W. W. ; DeLucas, L. J.; J. *Appl. Cryst.,* **1998**, 31, 515

(12)   Chayen, N. E.; *Trends in biotechnology,* **2002**, 20, 98

(13)   Stevens, R. C. *Current Opinion in Structural Biology,* **2000**, 10, 558

(14) Luft, J. R.; Collins, R. J.; Fehrman, N. A.; Lauricella, A. M.; Veatch, C. K.; DeTitta, G. T.; *Journal of Structural Biology*, **2003**, 142, 170

(15) Hosfield, D.; Palan, J.; Hilgers, M.; Scheibe, D.; McRee, D. E.; Stevens, R. C.; *Journal of Structural biology*, **2003**, 142, 207

(16) Watanabe, N.; Murai, H.; Tanaka, I., *Acta Cryst.*, **2002**, D58, 1527

(17) Walter, T. S.; Diprose, J.; Brown, J.; Pickford, M.; Owens, R. J.; Stuart, D. I.; Harlos, K., *Journal of Applied Crystallography*, **2003**, 36, 308

(18) DeLucas, L. J.; Bray, T. L.; Nagy, L.; McCombs, D.1 Chernov, N.; Hamrick, D.; Cosenza, L.; Belgovskiy, A.; Stoops, B.; Chait, A.; *Journal of Structural Biology*, **2003**, 142, 188

(19) Li, F. ; Yeung, E. S.; *Analytical and Bioanalytical Chemistry*, 2005, **83**, 1034

(20) McPherson, A., Crystallization of biological macromolecules, cold spring harbor laboratory press, 1999

(21) International Human Genome Sequencing Consortium; *Nature*, **2004**, 431, 931

Table 1   The recipe for all precipitants. The solutions shown in each row were prepared by the same buffer solution with different concentration of sodium chloride as shown in the top row.

Solution A is 0.1M sodium phosphate buffer with 0.1M sodium acetate at pH2.6;

Solution B is 0.1M sodium citrate buffer with 0.1M sodium acetate at pH3.6;

Solution C is 0.1M acetate buffer with 0.1M sodium acetate at pH4.6;

Solution D is 0.1M sodium citrate buffer with 0.1M sodium acetate at pH5.6;

Solution E is 0.1M sodium citrate buffer with 0.1M sodium acetate at pH6.6;

Solution F is 0.1M HEPES buffer with 0.1M sodium acetate at pH7.6;

Solution G is 0.1M TrisHCl buffer with 0.1M sodium acetate at pH8.6;

Solution H is 0.1M CHES buffer with 0.1M sodium acetate at pH9.6;

Solution I is 0.1M CAPS buffer with 0.1M sodium acetate at pH10.6;

	0.4M	0.6M	0.8M	1M	1.2M	1.4M	1.6M	1.8M	2M
2.6	A1	A2	A3	A4	A5	A6	A7	A8	A9
3.6	B1	B2	B3	B4	B5	B6	B7	B8	B9
4.6	C1	C2	C3	C4	C5	C6	C7	C8	C9
5.6	D1	D2	D3	D4	D5	D6	D7	D8	D9
6.6	E1	E2	E3	E4	E5	E6	E7	E8	E9
7.6	F1	F2	F3	F4	F5	F6	F7	F8	F9
8.6	G1	G2	G3	G4	G5	G6	G7	G8	G9
9.6	H1	H2	H3	H4	H5	H6	H7	H8	H9
11	I1	I2	I3	I4	I5	I6	I7	I8	I9

FIGURE CAPTIONS

Figure 1.   Photography of the liquid handling system. Center, 81 vials containing different precipitants. Center up, two 81-capillary boundless serving as inlet and outlet. Left, computer-controlled syringe pump. Right, capillary array head, 81-well sample plate and a small CCD camera used for alignment between the capillary head and the crystallization plate.

Figure 2.   The first picture shows 100nL different precipitants(100nL for each) were dispensed. The second picture shows 200nL each of different precipitants were dispensed.

Figure 3.   The 81-well fused silica crystallization plate is shown on the top. The bottom is the comparison of the crystallization plate, a penny coin and the traditional VDX 24-well plate.

Figure 4.   Photography of the detection system. Center top, water-cooled CCD camera. Center middle, quartz camera lenses. Other specific optic components are shown in Figure 3.

Figure 5.   The illustration of the detection system including both fluorescence and visible light detection schemes.

Figure 6.   The comparison of fluorescence image and visible light image of the same set of crystals. The top one is a visible light image and the bottom one is the fluorescence one. The crystal in the first well at the second row is an inorganic (NaCl) crystal. Exposure time: 300 sec.

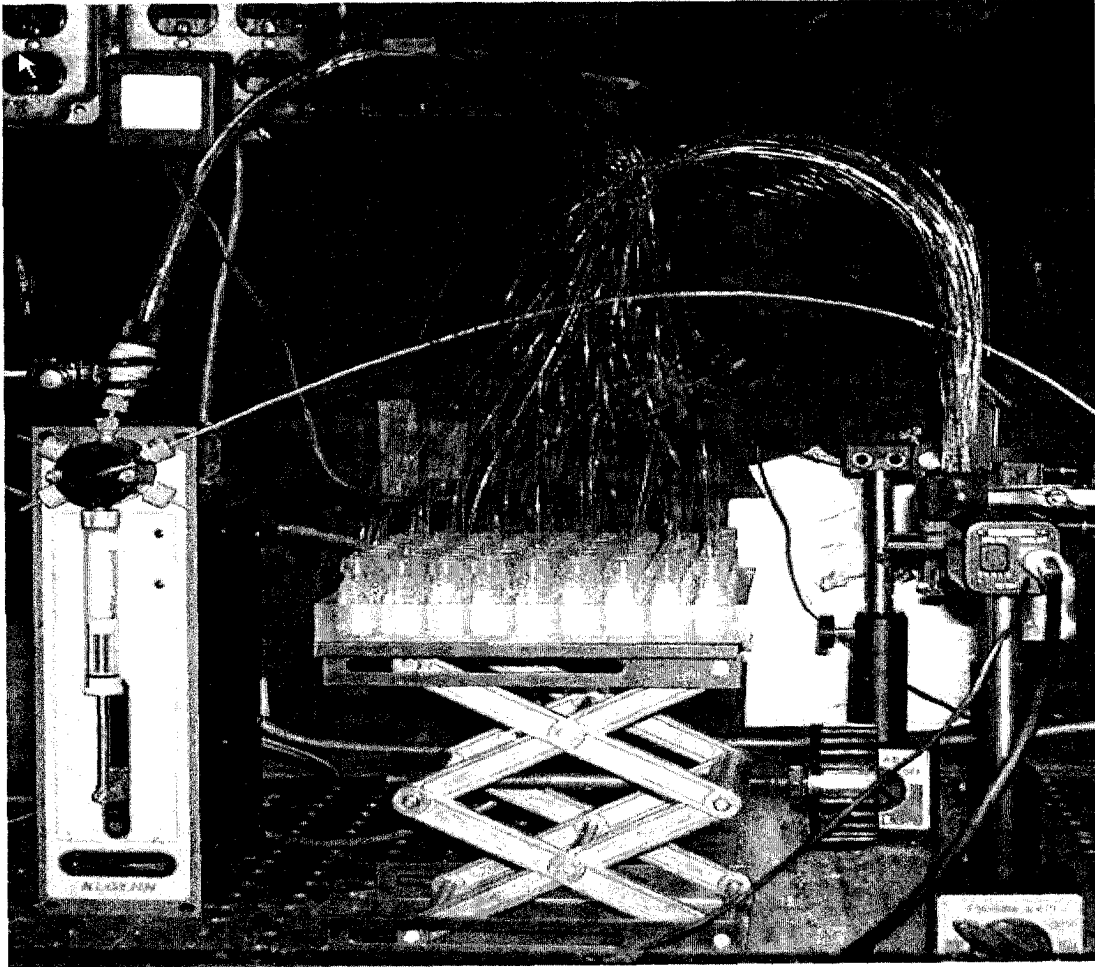Figure 7.   The image of crystals taken in the visible light detection mode. Exposure time: 20 sec.
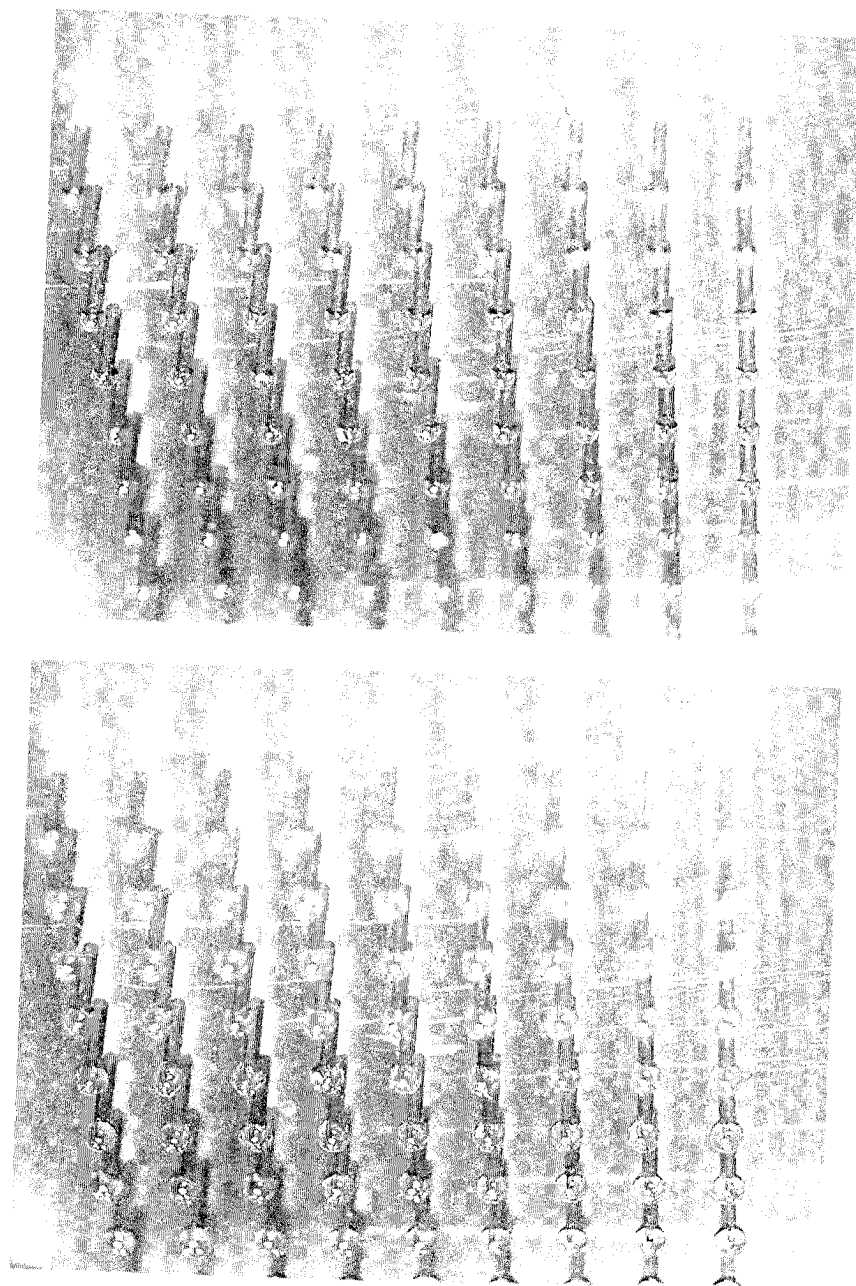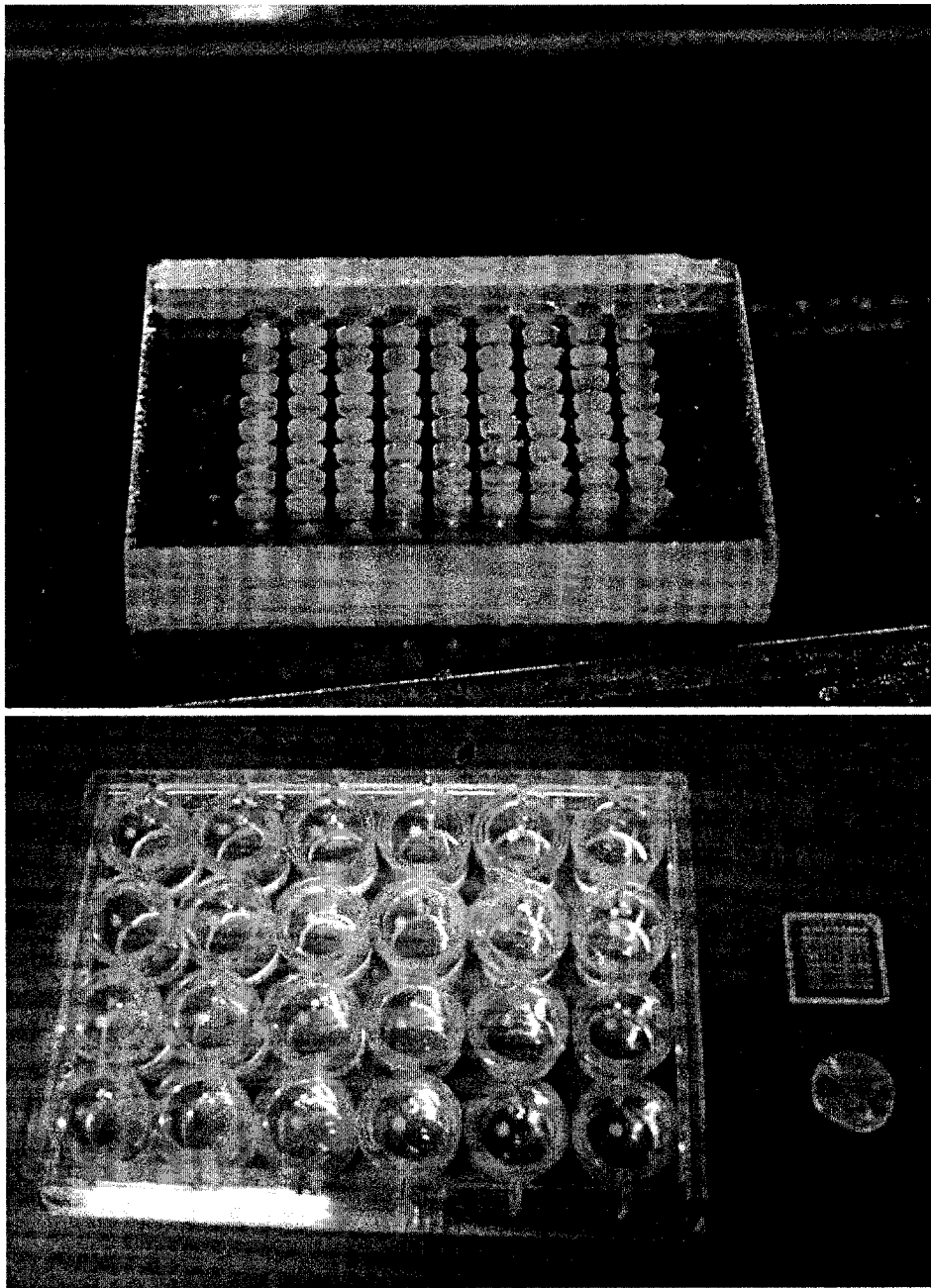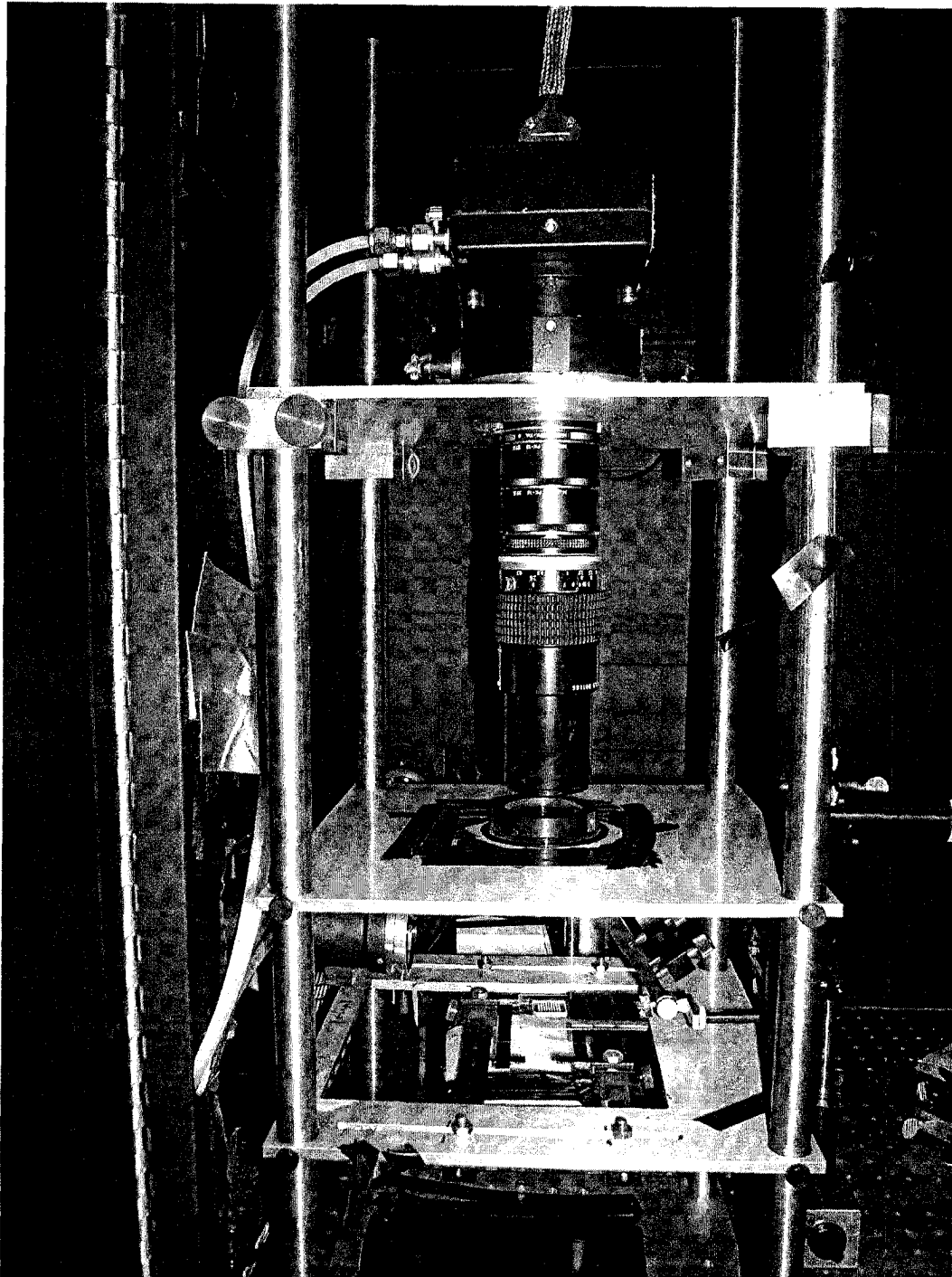
FIGURE 1
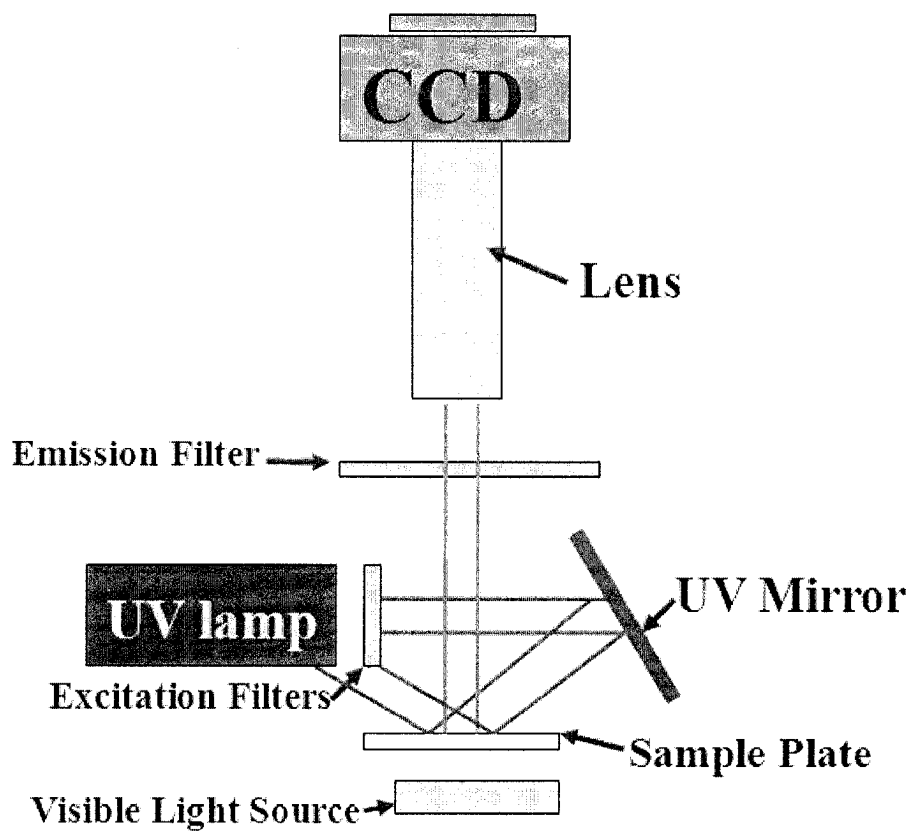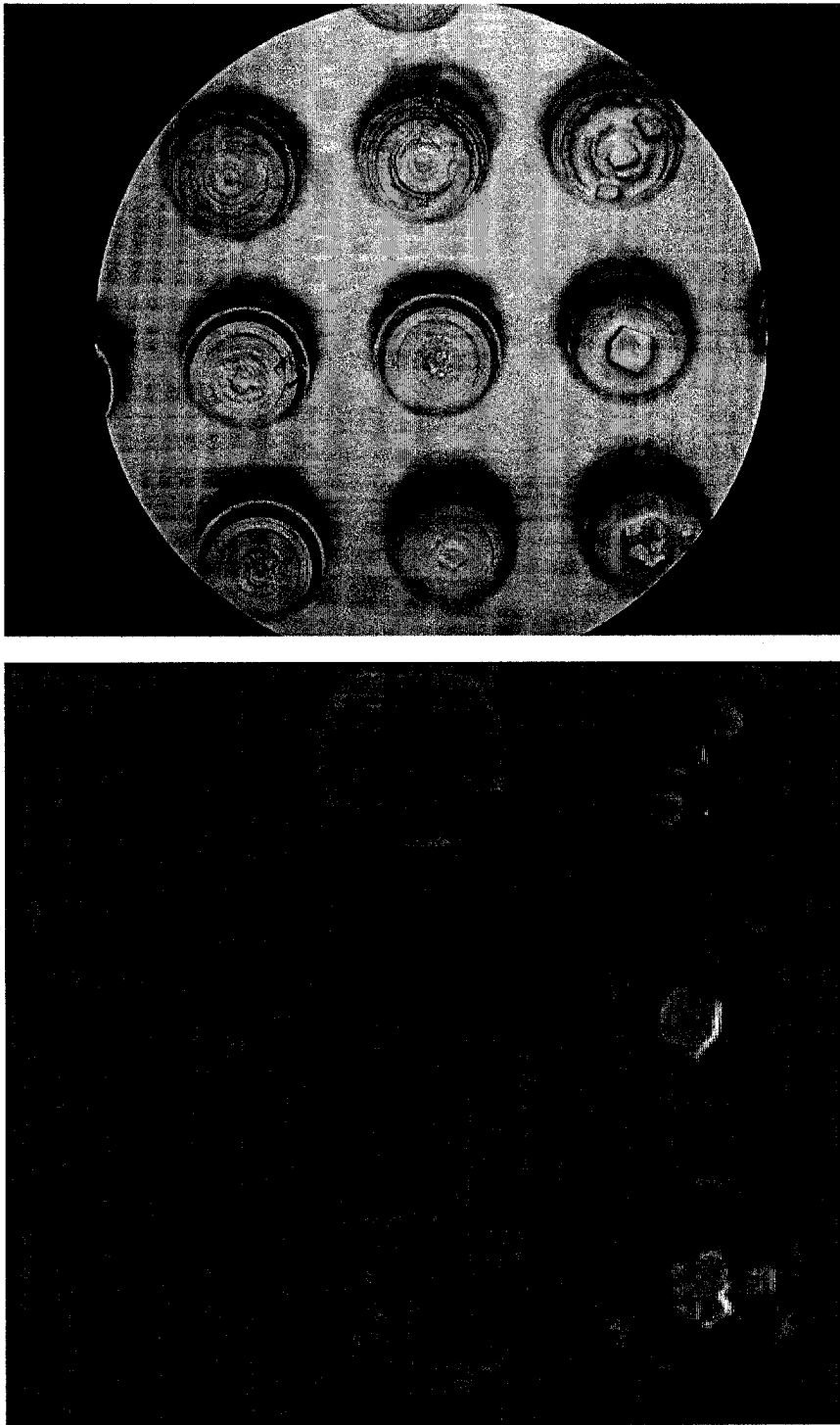
FIGURE 2

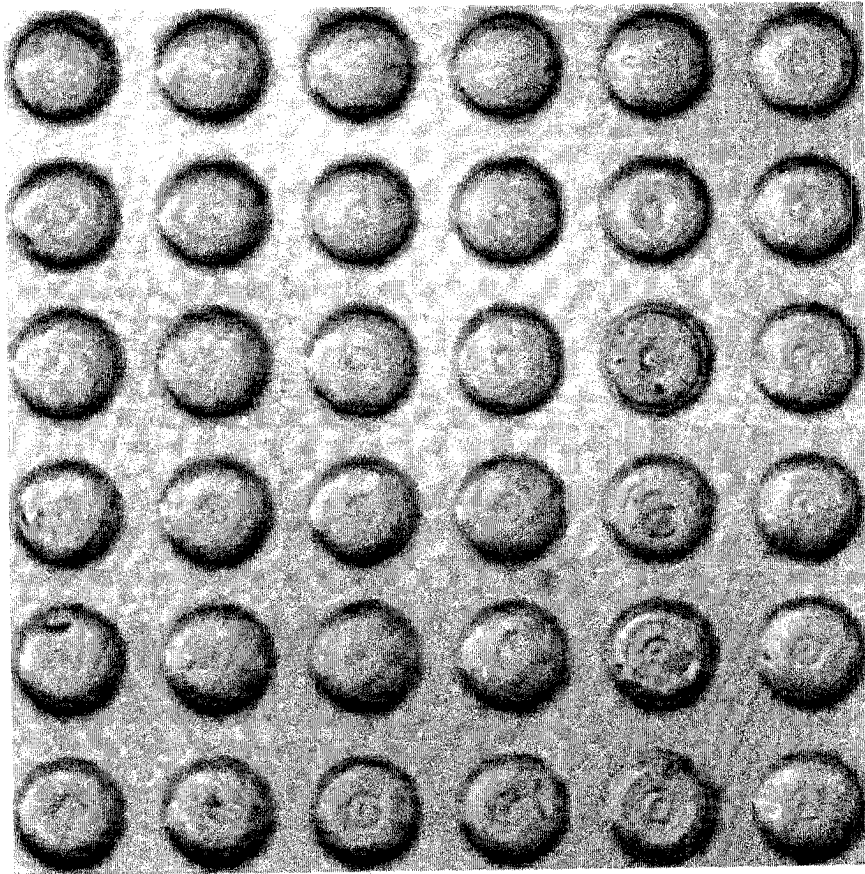FIGURE 3

FIGURE 4

FIGURE 5

FIGURE 6

FIGURE 7

CHAPTER 3 A NOVEL CRYSTALLIZATION METHOD FOR AUTOMATED, HIGH THROUGHPUT PROTEIN CRYSTALLOGRAPHY

Fenglei Li, Howard Robinson[1] and Edward S. Yeung

ABSTRACT

A new crystallization method highly amenable to automation and high throughput protein crystallography was developed. The novel crystallization mechanism by employing a gas permeable membrane to achieve the gentle evaporation required by protein crystallization was identified. Protein consumption is significantly reduced by employing only nanoliter protein solutions for each trial and by exploring more conditions in a phase diagram for each trial. The method provides the capability of evaporation control during the crystallization process, which can facilitate the nucleation and grown processes. The protein crystals gotten by this method were proven to possess high x-ray diffraction qualities. The method is also suitable for scale-up experiments.

---

[1] Biology Department, Brookhaven National Laboratory, Upton, NY 11973-5000

INTRODUCTION

Recently it is determined that the human genome comprises approximately 20,000–25,000 protein-coding genes [1]. The human proteome dictated by these genes will be about 30,000 to 100,000 proteins [2]. The structures and functions of most of them are unknown.

Knowing the three dimensional structures, especially all the key "functional" sites, of proteins can facilitate understanding on the relationship between structure, function and sequence of protein. Knowing the structures of protein target and the protein-ligand complex enables organic chemists to optimize the drug candidates in a more prompt and efficient way [4].

Structural proteomics or structural genomics has become more and more important recently as an important part of functional genomics, whose goals are to systematically and thoroughly study the distribution, modification and interaction of gene products in tissues [17].

Three techniques have been employed for protein structure determination: X-ray crystallography, nuclear magnetic resonance spectroscopy and mass spectrometry. X-ray crystallography has been the predominant and still remained as the only method for three dimensional structure determinations, at atomic resolution, of protein molecules with molecular weight larger than 30 000Da regardless of complexity [4].

In order to get the three dimensional structures of protein molecules by X-ray crystallography, diffraction quality protein crystals must be gotten. Most of the time, protein crystallization is one of the major "bottleneck" in the whole process of protein structure determination (which generally includes cloning, protein expression, purification, quality assessment, crystallization, synchrotron x-ray diffraction data collection and structure determination) [5].

The process of protein crystallization generally includes nucleation, crystal growth and cessation of growth. There are a lot of parameters influencing the crystallization process. It is very difficult to predict the growth conditions. The science of protein crystallization is an underdeveloped area. Protein crystallization is mainly a trial-and-error procedure.

Currently, people still rely on empirical method by screening a batch of conditions, which comprise a lot of sets of combination of pH, temperature, type and concentration of precipitant and additives and so on. Due to the large number and interdependence of all possible experimental parameters, an exponential explosion in the number of possible conditions to be tried occurs [12].

This kind of screening normally requires large amount of purified proteins (25-300mg). However, the availability of proteins is usually limited by the cost or resources associated with protein expression and purification [3].

Moreover, in this proteomic era, a huge number of new proteins need to be determined by x-ray crystallography. The goal of functional genomics approximately requires determination of about 16, 000 new protein structures which have been chosen as modeling templates to evenly cover protein space [10].

Therefore, it is critical to significantly reduce the amount of protein consumed in the high throughput screening [3] and to increase the degree of automation of the whole process in order to significantly increase the throughput of the whole profess of protein structure determination.

Therefore, miniaturization and automation are the two key factors in developing methodologies and instruments in order to realize high throughput for protein structural biology.

Currently, there are mainly two traditional methods employed for high throughput crystallization screening development: microbatch and vapor diffusion (hanging drop or sitting drop). Conventional crystallization trials typically use 1-2 uL of both protein and

reservoir solution in each hanging drop. Generally speaking, these two methods are executed by manual operations.

For reduction in the protein consumption, there are some efforts aiming to minimize these two methods. R. Stevens [15] proved as less as 20nL of both protein and reservoir solution can be used for the method of vapor diffusion to do protein crystallization. They showed[15] employing smaller volume of protein solutions not only requires less protein and in turn allows an increase in the screening of crystallization trails but also promotes faster vapor-diffusion mediated equilibration and thus decreases the overall time necessary for crystallization trials.

The consequence of that reduction in the time required for crystallization is a concomitant reduction in the degree of protein degradation by oxidation, deamidation, aggregation and denaturation, which is especially important for those proteolytically sensitive proteins [6]. G. DeTitta et al showed [16, 18] a miniaturized version of microbatch crystallization method, which can use as less as 200nL protein solutions.

To increase the throughput of protein crystallization screening by the traditional methods mentioned above, several groups have been developing automated systems which can perform fast and a large number of crystallization trials. G. DeTitta et al [18] reported an automated system which can perform 40,000 microbatch experiments per day. They use high-density microtiter plates to screen 1536 conditions for each protein. Syrrx, Inc. [6] developed an automated robotic crystallization system including a series of robotics workstations. This system can dispense nanoliter volumes of protein droplets (20-100 nL) at an increased rate of setting up a 96-well plate in 2 minutes for sitting-drop vapor diffusion protein crystallization screening experiment [6].

However, sophisticated and expensive robots have to be employed [6] because of the relatively complicated operation that the two traditional methods require. Therefore,

developing novel crystallization methods, which are highly compatible with automation and high throughput are highly desired.

Here, we report one new method for protein crystallization screening, especially suitable for automation and high throughput. It consumes very small amount of protein sample by reducing the amount of protein required for each trial and increasing the number of conditions one single trial can explore.

EXPERIMENTAL SECTION

Crystallization Plates

Two crystallization plates were employed for crystallization experiment in this work. Both of them were made of fused silica, which were purchased from Heraeus Optics, Inc. They were made by ultrasonic machining method because of their inherent properties of brittleness. One of them has totally eighty-one, nine by nine, small wells. The diameter of each well is 1.2mm and the spacing between wells is 500nm. The depth of each well is 2.5mm. The other one has twenty-five bigger wells. The diameter of each well is 2.4mm and the spacing is between wells is 750nm. The depth of each well is 3mm. The fused silica was purchased from Heraeus Optics, Inc. Before each use, the plate was carefully cleaned by an ultrasonic device.

Gas Permeable Membrane

The gas permeable membrane was originally designed for cell culture. It allows oxygen, carbon dioxide and water vapor to pass through. The moisture transmission rate is 700

grams per square meter per 24 hours with 100% relative humidity vapor contacting the adhesive underside of the membrane [7].

Liquid Dispensing System

The same liquid handling system has been employed and described in our previous work [11].The liquid handling system has the capability of aspirating or dispensing simultaneously different solutions from 20 nanoliter to approximately 24uL.

Materials and Reagents

Lysozyme was purchased from Seikagaku Corporation. CHES (N-cyclohexyl-2-aminoethanesulfonic acid), sodium citrate CAPS(N-cyclohexyl-3-aminopropanesulfonic acid), were purchased from Sigma. Sodium hydroxide, trisHCl (tris(hydroxyl)aminomethane hydrochloride), hydrochloric acid, sodium chloride, sodium acetate, HEPES (4-(2-hydroxyethyl)piperazine-1-ethanesulfonic acid sodium salt) (crystallization grade) were purchased from Hampton Research, Inc. Sodium phosphate was purchased from Fisher Scientific.

Lysozyme solutions were freshly prepared before each experiment by dissolving powders in the appropriate buffer and then centrifuged to get rid of any solid substances.

All buffers were freshly prepared by adding appropriate aliquots of concentrated components purchased from Hampton Research Inc., Fisher Scientific or Sigma. The pHs were adjusted by adding appropriate amount of 1M sodium hydroxide or 1M hydrochloric acid solution (crystallization grade, purchased from Hampton Research Inc.) and were confirmed by a calibrated pH meter.

RESULTS AND DISCUSSION

Protein Crystallization

In the vapor diffusion method (either hanging drop or sitting drop), the drop of the mixture of a protein and a precipitant solutions is equilibrated against the reservoir solution (the same as the precipitant in the drop but twice of the concentration), which results in a continuous concentration of the drop until the equilibrium is achieved [12]. The evaporation rate decreases with the difference in concentration of the precipitant decreasing [12]. The concentration of the protein and precipitant in the drop increases during the diffusion process. Therefore, each drop "sweeps" a range of conditions [13].

In the original microbatch method, the super saturation level is kept fixed from the beginning of mixing the protein and precipitant solutions until protein crystallizes out from the solution. So, one single trail of microbatch method "sweeps" less conditions than vapor diffusion method. Therefore, overall, microbatch method takes more trails, namely more protein and precipitant, to hit the right condition for protein crystallization.

Moreover, R. Stevens et al developed a modified vapor diffusion method which significantly decreases the amount of protein required by each single trial when vapor diffusion method is employed [15]. However, microbatch method is better than vapor diffusion method in terms of amenity to automation since the latter is involved more complicated operation and requires more sophisticated and expensive instrumentation [14].

Like vapor diffusion method, there is a trend to develop miniaturized microbatch methods, for example, G. DeTitta et al reported one modified microbatch method under oil which only requires 200nl protein sample [16, 18]. Despite the small protein consumption and good amenity to automation, microbatch method has the problem of the interaction

between the oil and the ingredients in the mother liquor such as some widely used organic precipitants and some small volatile organic molecules soluble in oil [15].

More importantly, in the microbatch method, since there is no a graduated concentration process as that in the vapor diffusion method, the direct mixing two high concentration solutions, the protein and precipitant solutions, can result in crystal showers or even precipitation [15]. Therefore, to develop a new method possessing the advantages of both vapor diffusion method and microbatch method is highly desirable.

There are some efforts on giving the capability of concentrating protein and precipitant to microbatch method have been reported [17, 18] by employing an oil layer of mixing two different types of oils such as silicon oil and paraffin oils.

Here, we reported a novel protein crystallization method which can not only significantly reduce the protein consumption, have the capability of exploring more conditions for each single trial, but also be very amenable to high throughput and automation. Similar to the vapor diffusion method, it has the concentrating capability and thus it explores a range of conditions in the phrase diagram.

Unlike the vapor diffusion method, our method does not stop the exploring process since it won't reach the equilibrium like the vapor diffusion method does. More importantly, unlike the vapor diffusion method, it does not require complicated mechanical operations and essentially eliminates the need of expensive robots for high throughput and automation. Since there is no oil layer in our method, there is no interaction between oil and the ingredients of protein crystallization solutions.

Figure 1 shows the crystallization plate used for demonstration of this new crystallization method. It is made of fused silica which can facilitate the fluorescence detection method we recently developed [11]. It could be made of glass or plastic or anything that is transparent if a regular transmitted light microscopy is employed as the detection method. For this particular plate, there are 81 individual micro wells which can hold 81

different crystallization mother liquors. A high throughput and automatic dispensing multiple different crystallization mother liquors had been achieved by a system described in our recent work [11]. After dispensing solutions to the wells, a sticky gas permeable membrane can be applied on the surface of the plate.

Figure 2 shows the configuration of the set up. In current experiment, 100 nL 50 mg/mL lysozyme and 100 nL precipitant were mixed together. Since the water molecules in the mother liquor can diffuse out via the small pores on the gas permeable membrane, a slow evaporation resulting in concentrating the crystallization mother liquors can thus be achieved. If proper conditions are hit, protein crystals will show up in the micro wells. Since the only operation here is to apply the membrane to the plate, the whole process is very amenable to automation. Moreover, there are no fundamental reasons which can limit the number of micro wells that can be made on the plate. Therefore, this method is essentially suitable for high throughput.

Since the gas permeable membrane is pseudo-transparent, a regular transmitted light microscope can be used directly for the detection. The membrane can also be peeled off to further facilitate the detection. We have shown [11] a fluorescence method can be employed as a complementary detection scheme to the regular transmitted light detection method for examining the protein crystallization screening results conducted on a fused silica plate. Therefore, this crystallization method is naturally amenable to multiple detection schemes and easy to achieve a better detection than other methods.

Figure 3 shows some excellent lysozyme crystals we got by this method.

X-ray Diffraction Experiment

The diffraction quality of the lysozyme crystals were examined by X-ray diffraction experiments. Figure 4 shows one diffraction map got from a lysozyme crystal crystallized by

our new method. The x-ray experiment was done on a beam line at Brookhaven National Lab synchrotron radiation source. The crystal diffracts to 1.35 angstrom.

This x-ray diffraction result proves the capability of our new method to generate well-ordered high quality protein crystals.

Evaporation Rate Control

Figure 5 shows the schematic drawing of the phase diagram of different crystallization processes by the traditional vapor diffusion method (AB), the standard microbatch method (G) and our new method (AB, AC, AD, AE, AF).

For the standard vapor diffusion method, once after the cover slip is closed, there is no control on the concentrating process, which is completely decided by the difference in vapor pressure between the drop and the reservoir solution. The concentrating process stops when equilibrium is reached. The process is showed as route AB. It's a "self-sweeping" process which screens more than one condition.

In the original microbatch method, the concentration of the protein and precipitant don't change much after being mixed at the beginning of the experiment until there are some protein crystallize out from the mother liquor. It follows a route like G in Figure 5. Only one condition is tested for each single trial. Therefore, compared with the standard vapor diffusion method, less space in the phase diagram is explored.

In our new method, depending on the relative rate of nucleation and evaporation, the actual process could take one of the different routes such as AC, AD, AE, AF showed in Figure 5, depending on the relative rate of evaporation and that of nucleation or crystallization of protein. Since the evaporation rate can be controlled by changing the pore sizes or distribution of pores, this new method allows different routes or more options for

exploring the phase diagram. This is important because this provides one more experimental parameter to vary in the crystallization screening experiments.

Figure 6 shows three experiments in which different number of membranes were applied to the crystallization plate. Since the gas permeable membranes are sticky, one membrane can be applied to another one to form a two-layer membrane or more layers. One layer of membrane shows fastest evaporation rate. Two-layer membrane shows slower evaporation and the three-layer one had the slowest rate. This shows the gas transportation rate of the membrane was changed and thus changed the crystallization process.

Therefore, to tailor the pore size of the membrane can essentially tailor the evaporation rate. Employing different membranes with different pore sizes at different stage of a crystallization process could essentially form a "evaporation gradient" which could allow a faster evaporation process at the very beginning and a slower evaporation rate for the later stage to facilitate the initial nucleation process and the later growth process since these two processes actually require different evaporation rates.

Moreover, one single trail of crystallization process could have different evaporation rates for its different stages. So, it's possible to form a "evaporation gradient" by employing a membrane with smaller pores first and later to switch to a membrane with bigger pores since it's so easy to physically change the membrane without bring much disturbance to the solutions in the wells.

Scale Up

Generally larger volume of mother liquor yields bigger crystals, which can diffract light more strongly and thus provide high resolution data [12]. Therefore, scale-up capability is very important for a crystallization method when it is employed for growing the final

crystals used for data collection. Larger crystals were obtained in larger volume by this method.

CONCLUSION

A new crystallization method was developed. It is highly amenable to automation and high throughput protein crystallography because of its inherent properties. It significantly reduces the protein consumption by using nanoliter solutions. It further reduces the total protein consumption by exploring more space in a phase diagram for each single trial. It provides one more parameter to take into control in crystallization screening experiments, which is the evaporation rate control. The protein crystals gotten by this method exhibits excellent x-ray diffraction quality. This method has also excellent scale up capability.

ACKNOWLEDGEMENT

REFERENCES

(1)   International Human Genome Sequencing Consortium; *Nature,* **2004,** 431, 931

(2)   Kempner, M. E., Felder, R. A., *Am. Genomic/Proteomic Technol.,* **2002,** 2, 6

(3)   Lawrence J. DeLucas, L.; Terry L. Bray; Lisa Nagy; Debbie McCombs; Nikolai Chernov; David Hamrick; Larry Cosenza; Alexander Belgovskiy; Brad Stoops; Arnon Chait; *Journal of Structural Biology*, **2003**, 142, 188

(4)   Blundell, T. L.; Jhoti, H.; Abell, C.; *Nature Reviews,* **2002**, 11, 45

(5)   Stevens, R., *Current opinion in Structural Biology,* **2000**, 10, 558

(6)   David Hosfield; John Palan; Mark Hilgers; Daniel Scheibe; Duncan E. McRee; Raymond C. Stevens; *Journal of Structural Biology*, **2003**, 142, 207

(7)   Product information, Diversified Biotech.

(8)   G. Juarez-Martinez et al, *Anal. Chem.*, **2002**, 74, 3505

(9)   Takamitsu Ikkai and Katsuhiko Shimada, *Journal of fluorescence*, Vol. 12, no.2, **2002**, 167

(10)   Heinemann, Udo; Bussow, Konrad; Mueller, Uwe; Umbach, Patrick; *Acc. Chem. Res,.* **2003**, 36, 157

(11)   Li, F.; Yeung, E.; Analytical and Bioanalytical Chemistry, 2005, 83, 1034

(12)   McPherson, A.; *Crystallization of biological macromolecules*, Cold Spring Harbor Laboratory Press, Cold Spring Harbor, New York, **1999**

(13)   Chayen, N. E.; *Acta Cryst.,* **1998**, D54, 8

(14)   Santarsiero, B. D.; Yegian, D. T.; Lee, C. C.; Spraggon, G.; Gu, J.; Scheibe, D.; Uber, D. C.; Cornell, E. W.; Nordmeyer, R. A.; Kolbe, W. F.; Jin, J.; Jones, A. L.; Jaklevic, J. M.; Schultz, P. G.; Stevens, R. C.; *Journal of Applied Crystallography*, **2002**, 35, 278

(15)   Christian A. Cumbaa, Angela Lauricella, Nancy Fehrman, Christina Veatch, Robert Collins, Joe Luft, George DeTitta and Igor Jurisica, Acta crystallographica. Section D, *Biological crystallography*, **2003**, D59, 1619

(16)   Udo Heinemann; Gerd Illing; Hartmut Oschkinat; *Current Opinion in Biotechnology* **2001**, 12, 348

(17)   Joseph R. Luft; Robert J. Collins; Nancy A. Fehrman; Angela M. Lauricella; Christina K. Veatch; George T. DeTitta; *Journal of Structural Biology*, **2003**, 142, 170

FIGURE CAPTIONS

Figure 1.   The images of the crystallization plate (a) and the plate covered by a gas permeable membrane (b)

Figure 2.   The schematic drawing of the configuration of each micro well on the crystallization plate.

Figure 3.   The images of lysozyme crystals crystallized by the new method.

Figure 4.   The X-ray diffraction map of a lysozyme crystal crystallized by our new crystallization method.

Figure 5.   The schematic drawing of a protein phase diagram. AB represents the route which a protein crystallization process by standard vapor diffusion method takes. G shows the route taken by a standard microbatch method. AC, AD, AE or AF represents respectively the possible routes taken by our new crystallization method.

Cstart is the concentration the mother liquor at the starting point of the crystallization experiment.

Cfinal is the final concentration of the mother liquor when the crystallization process is stopped.

Cp,start is the concentration of the protein solution at the starting point of the experiment.

Cp,final is the concentration of the protein solution at the final point of the crystallization process.

Figure 6.   The images of lysozyme crystals crystallized under different conditions. (a) one membrane layer (b) two membrane layers (C) Three membrane layers.

(a) 2 uL (1 uL 50 mg/mL lysozyme + 1 uL precipitant B7)

(b) 4 uL (2 uL 50 mg/mL lysozyme + 2 uL precipitant B7)

(c) 6 uL (3 uL 50 mg/mL lysozyme + 3 uL precipitant B5)

(d) 8 uL (4 uL 50 mg/mL lysozyme + 4 uL precipitant B7)

Protein: 50 mL/mL lysozyme

Precipitant:

B7: 1.6 M NaCl in 0.1 M sodium citrate buffer with 0.1 M sodium acetate at pH 3.6;

B5: 1.2 M NaCl in 0.1 M sodium citrate buffer with 0.1 M sodium acetate at pH 3.6;
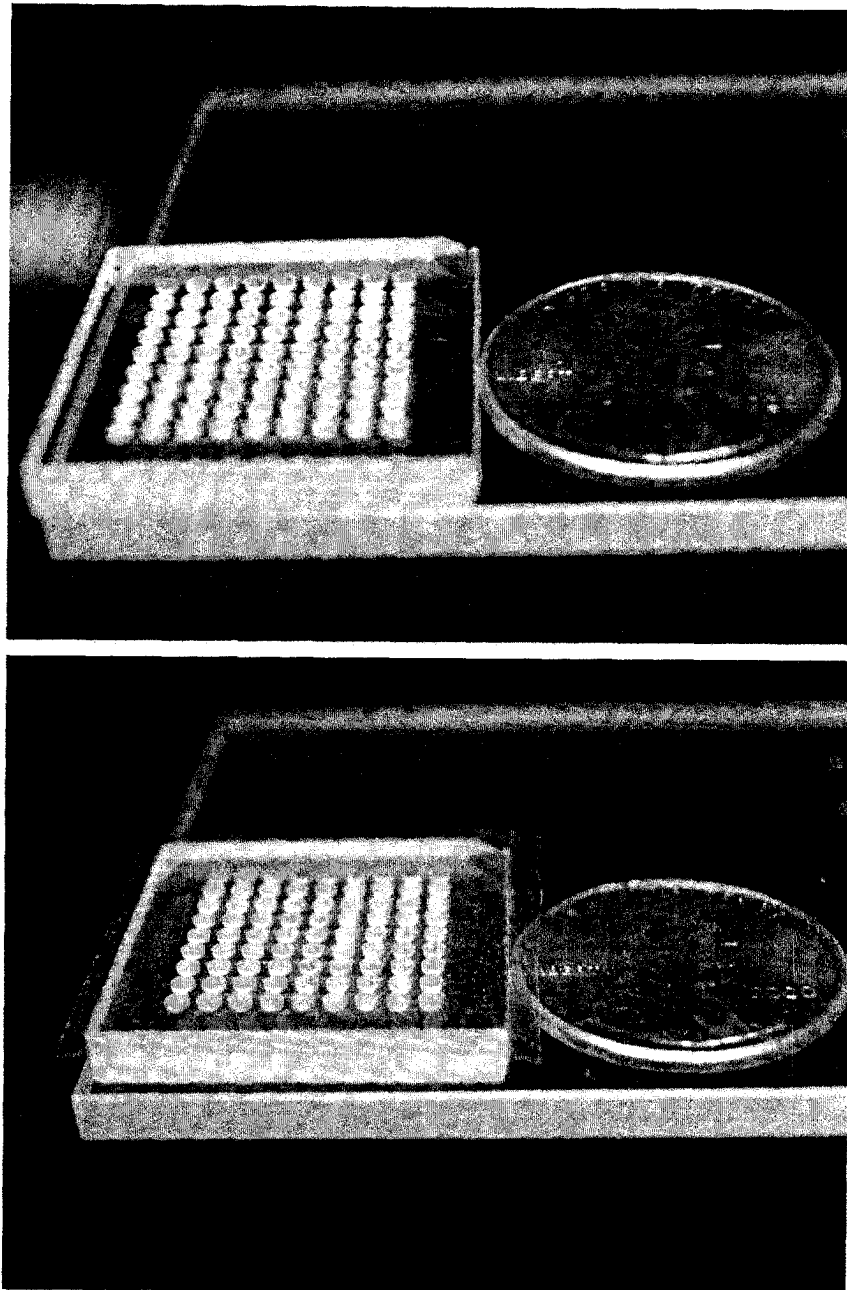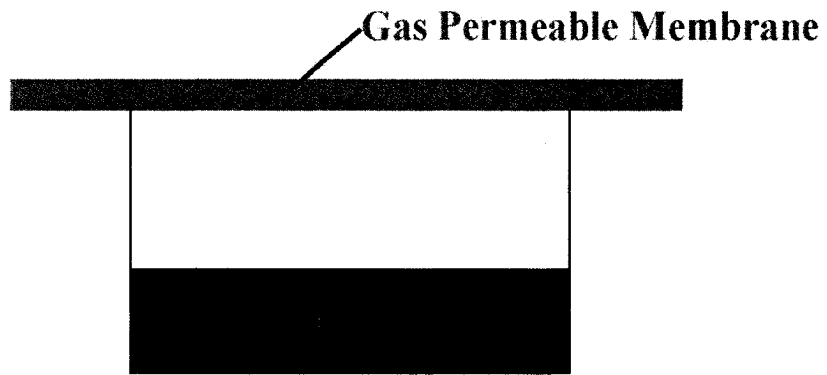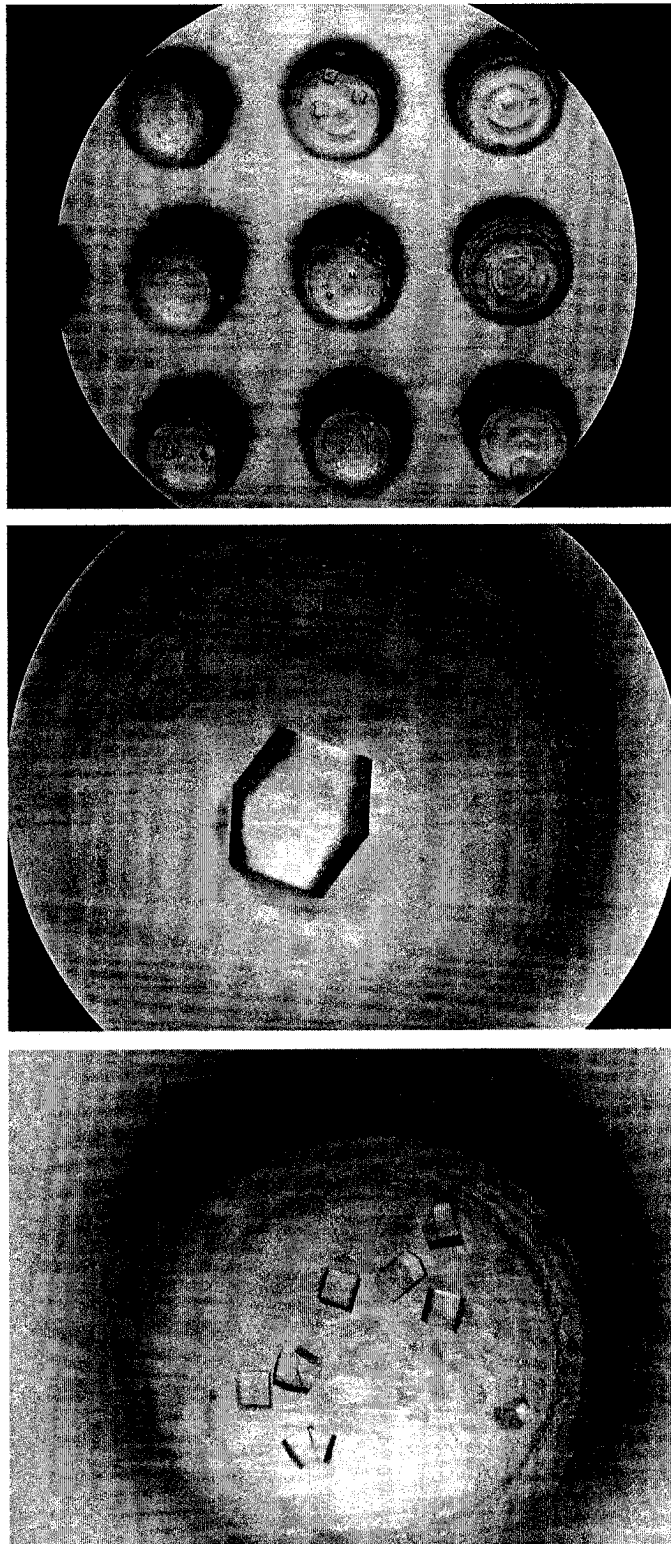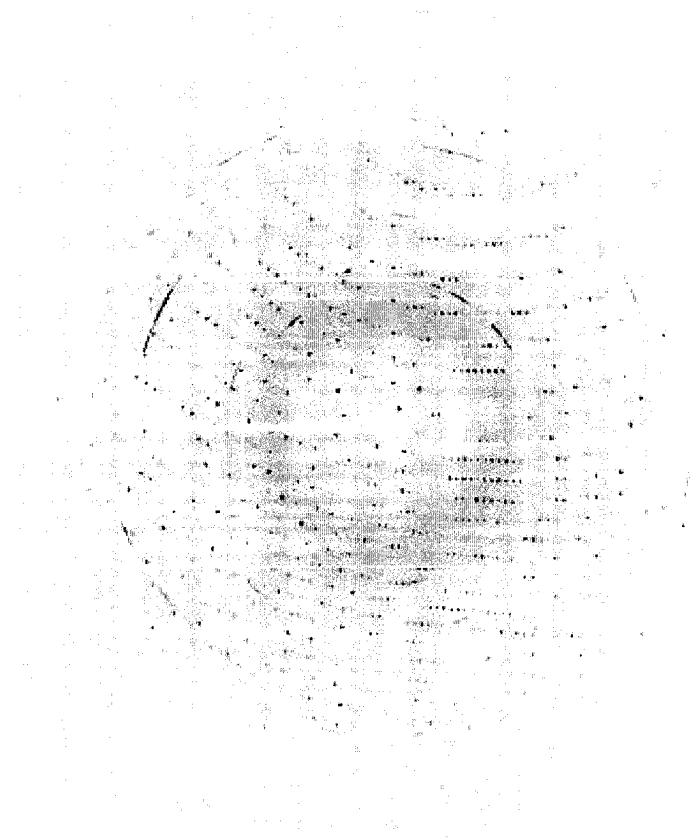
Figure 1
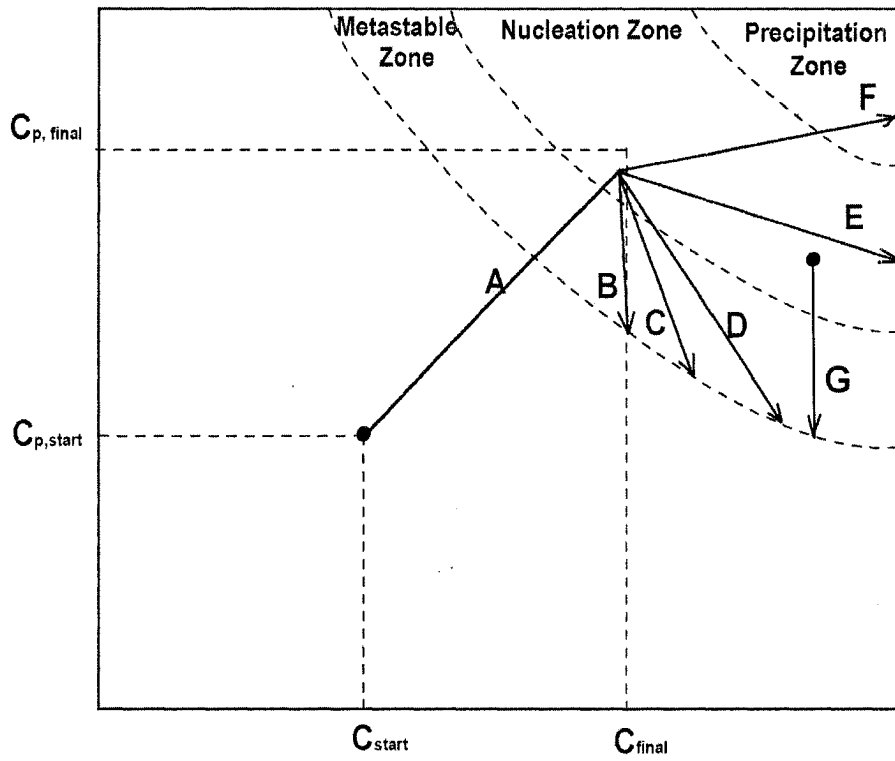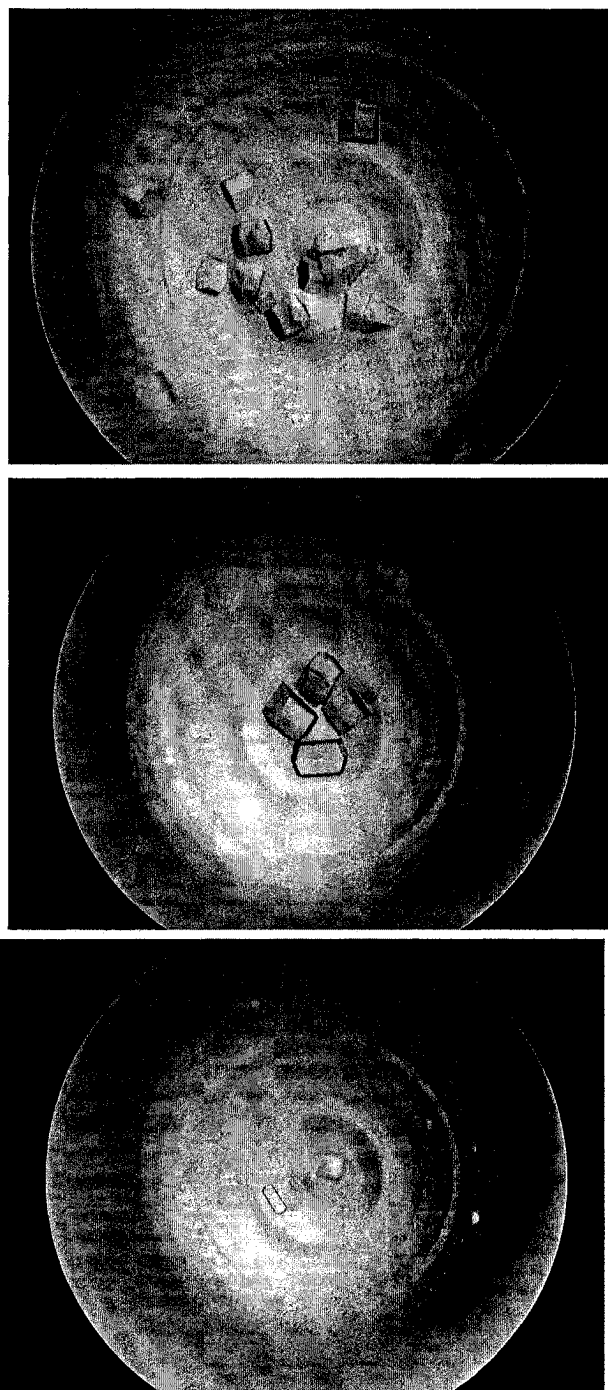
Figure 2

Figure 3

Figure 4

Figure 5

Figure 6

CHAPTER 4 STRUCTURE DETERMINATION OF HUMAN LACTATE DEHYDROGENASE COMPLEXED WITH NADH BY X-RAY CRYSTALLOGRAPHY

Fenglei Li, Howard Robinson[2] and Edward S. Yeung

ABSTRACT

Lactate dehydrogenase plays a vital role in crucial glycolysis in many species. Human lactate dehydrogenase 1 (H4) complexed with NADH was crystallized and x-ray diffraction data were collected with the best resolution at 2.5 A. The structures were solved by molecular replacement.

The structure of LDH/NADH displays significantly different structural features compared with that of LDH/NADH/inhibitor in that some subunits in LDH/NADH show open conformation or two conformations while the subunits in LDH/NADH/inhibitor show all close conformation.

---

[2] Biology Department, Brookhaven National Laboratory, Upton, NY 11973-5000

Multiple LDH/NADH crystals were obtained and employed for x-ray diffraction experiments. Difference in subunit conformation was observed in the structures independently solved from multiple individual LDH/NADH crystals.

Structural differences observed among crystals suggest the existence of multiple conformers in solution.

INTRODUCTION

Lactate dehydrogenase (LDH) had been found in many species from mammal and plants to bacteria [1]. LDH catalyzes the reversible oxidation of lactate to pyruvate with concomitant interconversion of coenzyme NADH to NAD+. NAD+ is required for glyceraldehydes-3-phosphate to be oxidized to 1,3-biphophoglycerate during glycolysis for production of ATP. The reaction LDH catalyzes serves as an important biological means in many species to regenerate NAD+ from NADH for glycolysis to produce energy under anerobic conditions.

In animal, LDH exists as a tetramer in a 222 symmetry. Each of the four subunits of LDH could be one of the two types of genetically distinct subunits: M, H, whose corresponding genes are LDH-A, LDH-B respectively. Therefore, LDH exists in five isozymes resulting from the hybridization of H and M subunits. LDH (H4) is usually found predominant in mainly anaerobic tissues such as cardiac muscle while LDH (M4) is the major form in anaerobic tissues such as skeletal muscle and liver [5]. In addition, there is the third type LDH , the X form, corresponding to the LDH-C gene and usually found in animal testes. Different isozymes have different kinetic properties [1].

Structures of LDH from various species such as pig, dog fish, human, mouse, Bacillus stearothermophilus, bifidobacterium and Plasmodium falciparum have been determined by x-ray crystallography.

The catalytic mechanism of LDH has been studied by various methods such as fluorescence polarization, fluorescence quenching spectroscopy, stop-flow kinetics and mutagenesis [1, 3]. A compulsory order of substrate binding with coenzyme first was identified. Although series of steps were suggested for the reaction, the rate-limiting step has not been well determined.

Based on the comparison between the structure of dog fish apoenzyme LDH M4 and that of an abortive ternary complex of LDH/NAD/pyruvate , the conformational change in the ternary complex was proposed to be induced by the coenzyme binding [2]. Later on, based on the information obtained from mutagenesis study [3, 17], the conformational change was proposed to be induced by the substrate binding for the case of LDH from Bacillus stearothermophilus [3]. The structure of apoenzyme LDH-C from mouse was found to be very similar to other LDH structures, surprisingly, however, the active site loop in this apoenzyme resembles not the "open" conformation found in apoenzyme dog fish LDH M4 structure but the "induced" "close" conformation found in the ternary LDH complex structures [4].

For the medical importance, Human LDH has been crystallized in the forms of H4 and M4 complexed with NADH and an inhibitor, oxamate [5]. The conformations of the active site loops in these two structures are all "close" as in the case of dogfish and porcine LDH[2].

To ultimately elucidate the reaction mechanism, structures of LDH in those important steps during the reaction coordinate could be of great value. However, in the current inventory of structures of LDH from mammal, there is no LDH/NADH binary structure yet.

This is largely because of the experimental difficulties of crystallizing LDH/NADH binary complex. However, valuable information regarding the active site could be missing because of the existence of inhibitor in the ternary complex since inhibitor has been thought to make the crystallization process easier by making LDH structure more rigid and thus the inhibitor could play a role in forming the ternary complex structure.

With the high throughput capability of the screening method we have recently developed [13], we were able to screen a large number of crystallization conditions and successfully crystallize the LDH/NADH binary complex.

In addition, our previous single molecule enzymatic kinetics study [9] suggests studying LDH and its binary complex with the coenzyme could reveal important information on the solution properties of protein molecules in terms of structure and function relationship.

EXPERIMENTAL SECTION

Materials and Chemical reagents

Highly purified, isozyme grade lactate dehydrogenase 1 from human heart (H4-hLDH) was purchased from Calzyme, Inc. NADH were purchase from Sigma. Crystallization grade sodium chloride, Tris (hydroxymethyl) aminomethane Hydrochloride, PEG 400, PEG 6000 were purchased from Hampton Research Inc.

Crystallization of Lactate Dehydrogenase

Lactate dehydrogenase was dialyzed for changing buffer, removing excess salt and increasing concentration to favor the thereafter crystallization experiments. LDH was dialyzed in 10 mM TrisHCl, 50 mM NaCl buffer in cold room for 30 hours.

LDH crystals were grown by hanging drop vapor diffusion method at room temperature. Six crystals of H4-hLDH were obtained by mixing equal volumes (2uL each) of a protein solution comprising 20 mg/mL H4-hLDH and 5mM NADH in 10mM TrisHCl, 50mM NaCl at pH 8.0 and a well solution containing 20% PEG 4000 and 60% PEG 400 in 0.20M TrisHCl at pH 8.1. One crystal of H4-hLDH was obtained by mixing equal volumes (2uL each) of a protein solution comprising 20 mg/mL H4-hLDH and 5mM NADH in 10mM TrisHCl, 50mM NaCl at pH 8.0 and a well solution containing 16% PEG 4000 and 60% PEG 400 in 0.20M TrisHCl at pH 8.1. Crystals were blocks or rods of various approximate dimensions ~100um x ~50um x ~60um.

Data Collection

Crystals of H4-hLDH were flash cooled to liquid nitrogen temperature in their original crystallization mother liquor without adding anything else. X-ray diffraction experiments were done in a synchrotron beam at Brookhaven National Laboratory. The data were processed using HKL2000. Crystals were of P212121 symmetry. There is one homotetramer in the asymmetric unit.

Structure Determination

The structures of H4-hLDH were solved independently from seven independent x-ray diffraction data sets from seven crystals named as E, F, G, J, K, N, R. Seven structures were solved independently by molecular replacement with AMORE [6]. Graphical images of the structures were created by Pymol [10].

The coordinates of a homotetramer of human LDH/NADH/oxamate were employed as a search model [5]. The molecular models were improved by refinements with CNS[7] and Xtalview [9]. Each subunit was treated independently throughput the refinement. The summary of final refinement statistics are shown in Table I.

RESULTS AND DISCUSSION

Comparison of LDH/NADH and LDH/NADH/inhibitor structures

Overall structures

Human lactate dehydrogenase 1 (H4) is a homotetramer with 332 amino acid residues in each subunit and a molecular weight of 146K (formula weight 36559.6 for each subunit). In LDH/NADH complex, each subunit has an active site where it binds one NADH. The four active sites in H4 LDH from some species have been found to be independent, noninteracting binding sites [1] .

Figure 1 shows the biological tetramer structure of H4 hLDH complexed with NADH at 2.5 A resolution determined by x-ray crystallography from the crystal named as "G". In this crystal structure, there is one homotetramer in each asymmetric unit. There is one NADH bound to each subunit. The space group is P212121. A summary of the crystallographic refinement is shown in Table I.

The global characteristic of this structure is similar to those of LDH complexed with other ligands and inhibitors. Extensive secondary structures are found in this enzyme. Amino acid residues located in the helices account for approximately 40% of the total residues. Beta structures are responsible for approximately 23% of total residues [1]. As in the structures of LDH from human (LDH/NADH/inhibitor) and other mammalian species, in each subunit, there are two domains formed by residues 20-162, 248-266 and 163-247, 267-331 [5]. The active site or substrate binding site is at the interface of the two domains. Six strands of parallel beta sheets form the NADH binding domain. As part of the domain, Residues 99-110 form a loop which plays an important role in NADH, substrate binding and LDH catalytic reaction.

For human lactate dehydrogenase 1 (H4), despite the large resemblance in global structure (Figure 2), in this study, a striking difference in terms of conformation of the active

site loop has been observed between the structures we determined from hLDH/NADH complex and those structures from LDH/NADH/inhibitor complex [5] . All active site loops (residues 99-110) in the four subunits are "closed" conformations in the human H4 hLDH/NADH/inhibitor structures [5]. However, in the LDH/NADH structures we have determined from multiple crystals in this study, we found the active site loops are not always in closed conformations. In some subunits, the conformation of the active site loop is closed while in others it is either open or two-conformation (open and closed).

Subunits with close conformation

In the hLDH/NADH structure determined from crystal G, the conformation of the active site loop (formed by residues from 99 to 110) in subunit A, B, C and D is found to be two-conformation, closed, two-conformation, closed respectively.

Figure 3 shows the closed conformation found in the subunit B of the structure determined from crystal G. Superposition of this structure with the structure of hLDH/NADH/inhibitor (Figure 4) shows the overall structural features are about the same. Those important residues located in the active site which are involved in catalytic reaction such as His 193, Arg 107, Arg 99 are in about the same positions. The coenzyme NADH is also located in about the same position.

Subunits with open conformation

Crystal K was obtained in the same drop (crystallization mother liquor) and was thus crystallized at exactly the same crystallization condition as crystal G. Two independent x-ray diffraction experiments were done on the two crystals and two data sets were independently processed.

Overlaying Subunit A Crystal K with Subunit B Crystal G shows overall resemblance except one striking difference that the active site loop is in an open conformation in Subunit A Crystal K (shown in Figure 5) rather than a close conformation as shown in Subunit B Crystal G. In the open conformation, the active site loop is extended towards solvent and the distance between Glu 102 and its corresponding position in close conformation is more than 10 angstrom. Both Arg 99 and Arg 107, the former related to NADH binding and the latter involved in stabilizing transition state [11] in the catalytic reaction, are located in this active site loop, therefore their positions are significantly different from those in a close conformation.

In the structure of human H4 LDH/NADH/inhibitor, Arg 99 forms a hydrogen bond with the pyrophosphate of NADH and the guanidinium group of Arg 107 is within hydrogen bonding distance of both the reactive carbonyl of pyruvate and imidazole ring of the catalytic His 193 as in the structures of LDH from other species [3]. These interactions were thought to be important for the catalytic reaction in the way of stabilizing either substrate or transition state complex [3]. The observation that the position of 193 in an open conformation is the same as in a close one may indicate this residue is independent from substrate binding. It may be also independent of the conformation of the active site loop since its position is the same for both open and close conformation.

Subunits with two conformations

More interestingly, Subunit C Crystal G shows both open and close conformations. In the electron density map (Figure6], in Subunit C Crystal G, the magnitude of the loop electron density in open conformation is estimated to be similar to that in the close one, but it is approximately half of that in Subunit B Crystal G. Moreover, the magnitude of the electron density of NADH in Subunit C Crystal G is about the same as that in Subunit B Crystal G.

This suggests the existence of two conformation in Subunit Crystal G is independent on the amount of NADH bound.

Comparison of multiple LDH/NADH structures

To compare the structures from different crystals, subunit A in K and subunit B in G are overlaid as shown in Figure 6. Most parts of the two structures are similar and can be overlapped well, but the two loops show significant difference as large as 10 A.

Figure 7 is the superposition of subunit B in K and subunit B in G. Both subunits have close conformations and the difference in these two subunits are inappreciable.

The heterogeneity in loop conformation existing in one crystal and among multiple crystals could result from (1) sequence (2) crystallization conditions (3) amount of NADH complexed with LDH (4) crystal packing. They are discussed as follows:

Sequence

The LDH in this study is a homotetramer. All crystals came from the same crystallization experiment and thus all crystals come from the same LDH solution. Therefore, all the sequences of the subunits should be the same.

Crystallization conditions:

Since both crystal G and crystal K were obtained from the same drop of crystallization mother liquor, crystallization condition is thus unlikely the reason.

Amount of NADH complexed with LDH

In crystal G, the amount (electron density) of NADH in Subunit B is about the same as that in subunit C. B shows one single close conformation, but C has two conformations.

In crystal K, the amount of NADH in subunit A, which is an open conformation, is lower than NADH in other subunits in crystal K. It may seem the low amount of NADH is responsible for the open conformation. However, in crystal F (also crystallized at the same condition), NADH in subunit A is lower than that in other subunits, but subunit A is in two-conformation and the electron density of the close conformation is stronger than the open one. Therefore, amount of NADH complexed with LDH is not correlated with a loop conformation.

Crystal Packing

If the difference in conformation results from crystal packing, then all the subunits located in the same location in the asymmetric unit should have the same conformation. However, this is not the case for the structures discussed here. For example, in crystal G, the conformations of four loops are two-conformation, close, two-conformation and close respectively. However, in crystal K, the conformations of subunits located at the corresponding positions are open, close, two-conformation and two-conformation. Two crystals have the same arrangement for the subunits in the asymmetric unit. Since the same location in the asymmetric unit doesn't lead to the same conformation, crystal packing should not the reason for the heterogeneity in loop conformation.

Based on the analysis above, the existence of heterogeneity of loop conformation is seemingly due to the inherent properties of LDH itself, i.e. LDH may exists in multiple conformations in solution. Moreover, if the different conformers are in a fast equilibrium as suggested by traditional protein solution thermodynamics, the loop would not have been seen

in an x-ray crystal structure because of the time-averaging nature of the technique. Therefore, those conformers should be long-lived species in solution.

CONCLUSION

Human lactate dehydrogenase 1 complexed with NADH was successfully crystallized without adding any inhibitor and the best resolution of x-ray diffraction data is 2.5A. Heterogeneity in conformation of the active site loop has been observed among subunits in the same crystal and among multiple crystals. Existence of long-lived LDH conformers in solution is suggested.

ACKNOWLEDGEMENT

REFERENCES

(1)   Boyer, P., The enzymes 3rd ed. Vol. XI, *Academic Press*, **1975**, 191

(2)   Margaret J. Adams, Manfred Buehner, K. Chandrasekhar, Geoffrey C. Ford, Marvin L. Hackert, Anders Liljas, Michael, G. Rossmann, IRA E. Smiley, William S.

Allison, Johannes Everse, Nathan O. Kaplan and Susan S. Taylor, Proc. *Nat. Acad. Sci* USA, **1973**, vol. 70, (7) p1968-1972

(3) Anthony R. Clarke, Dale b. Wigley, William N. Chia, David Barstow, Tony Atkinson and J. John Holbrook, *Nature*, **1986**, vol 324, p699-702

(4) Holly H. Hogrefe, James P. Griffith, Michael G. Rossmann and Erwin Goldberg, the *Journal of Biological Chemistry*, **1987**, v262, p13155-13162

(5) J. A Read, V. J. Winter, C.M. Eszes, R.B. Sessions and R.L.Brady, *PROTEINS: Structures, Function, and Genetics*, **2001**, 43, 175-185

(6) Navaza J. *Acta Crystallogr*, **1994**, A50:157-163

(7) A.T.Brunger, P.D.Adams, G.M.Clore, W.L.Delano, P.Gros, R.W.Grosse-Kunstleve, J.-S.Jiang, J.Kuszewski, M.Nilges, N.S.Pannu, R.J.Read, L.M.Rice, T.Simonson, G.L.Warren, *Acta Crystallographica Section D: Biological Crystallography*, **1998**, 54:901-21,

(8) Reginald H. Garrett and Charles M. Grisham, *Biochemistry, Saunders College Publishing, 2nd edition*, **1999**

(9) Qifeng Xue and Edward S. Yeung, *Nature*, **1995**, 373, 681 – 683

(10) D.E. McRee, *J. Molecular Graphics*, **1992**, Vol.10, pp. 44-46.

(11) Warren L. DeLano, DeLano Scientific LLC, San Carlos, CA, USA. http://www.pymol.org

(12) Clarke A. R., Dafforn, T. R., *Comprehensive biological catalysis: a mechanistic reference. (Sinnott M, ed.). New York: academic press*, **1998**, Vol III, p1-80

(13) F. Li, Howard Robinson and Edward S. Yeung, *Analytical and Bioanalytical Chemistry*, **2005**, 83(7-8), 1034-41

(14) Christian A. Cumbaa, Angela Lauricella, Nancy Fehrman, Christina Veatch, Robert Collins, Joe Luft, George DeTitta and Igor Jurisica, *Acta crystallographica. Section D*, **2003**, D59, 1619-1627

(15) Udo Heinemann; Gerd Illing; Hartmut Oschkinat; *Current Opinion in Biotechnology* **2001**, 12, 348-354

(16) Joseph R. Luft; Robert J. Collins; Nancy A. Fehrman; Angela M. Lauricella; Christina K. Veatch; George T. DeTitta; *Journal of Structural Biology*, **2003**, 142, 170-179

(17) A. R. Clarke, T. Atkinson and J. John Holbrook, *Trends Biochem. Sic.*, **1989**, 14, 101-105

Table 1. The resolutions of seven x-ray diffraction data sets collected on seven individual crystals and corresponding R factors and R free.

	e	f	G	j	K	n	r
Resolution	2.9	2.8	2.5	2.8	2.6	3	2.8
R	.2284	.2267	.2194	.2307	.2369	.2311	.2301
R free	.3166	.3101	.2790	.3172	.3027	.3140	.3156

FIGURE CAPTIONS

Figure 1.   This is the biological tetramer of LDH from crystal G. Each subunit is labeled by a different color.

Figure 2.   Superposition of crystal G (in green) with 1I0Z (in red).

Figure 3.   Loop (residue 99-109 shown in green) subunit B of crystal G. NADH is shown in blue. The loop has a close conformation.

Figure 4.   Superposition of Subunit B, Crystal G (green) with Subunit A, LDH/NADH/oxamate (red, 1I0Z)

Figure 5.   Subunit A of crystal K is shown in red, open conformation. NADH is in blue.

Figure 6   Electron density map of Subunit C of Crystal G: two conformations

Figure 7   Superposition of subunit A in K (red) and subunit A in G (green)

Figure 8.   Superposition of subunit B in K (red) and subunit D in G (green)
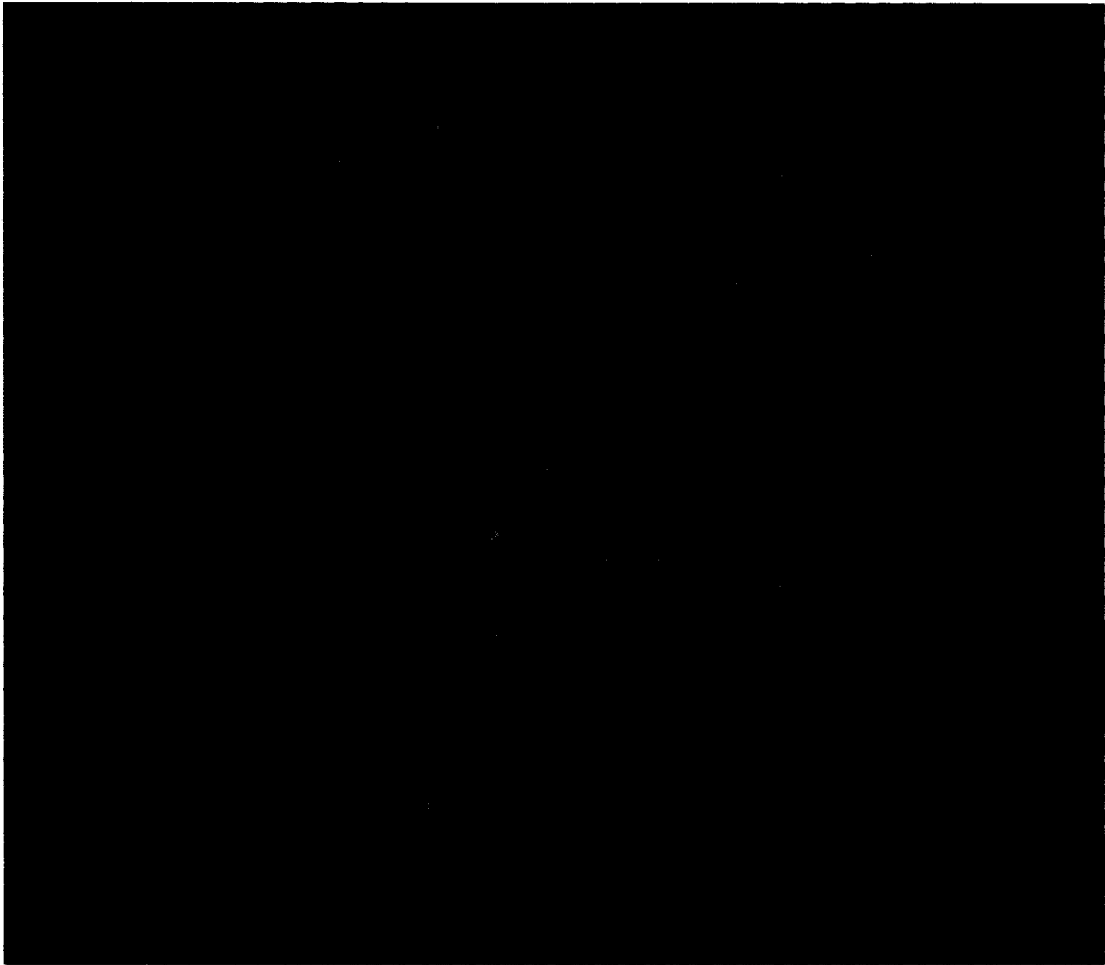
Figure 1

Figure 2
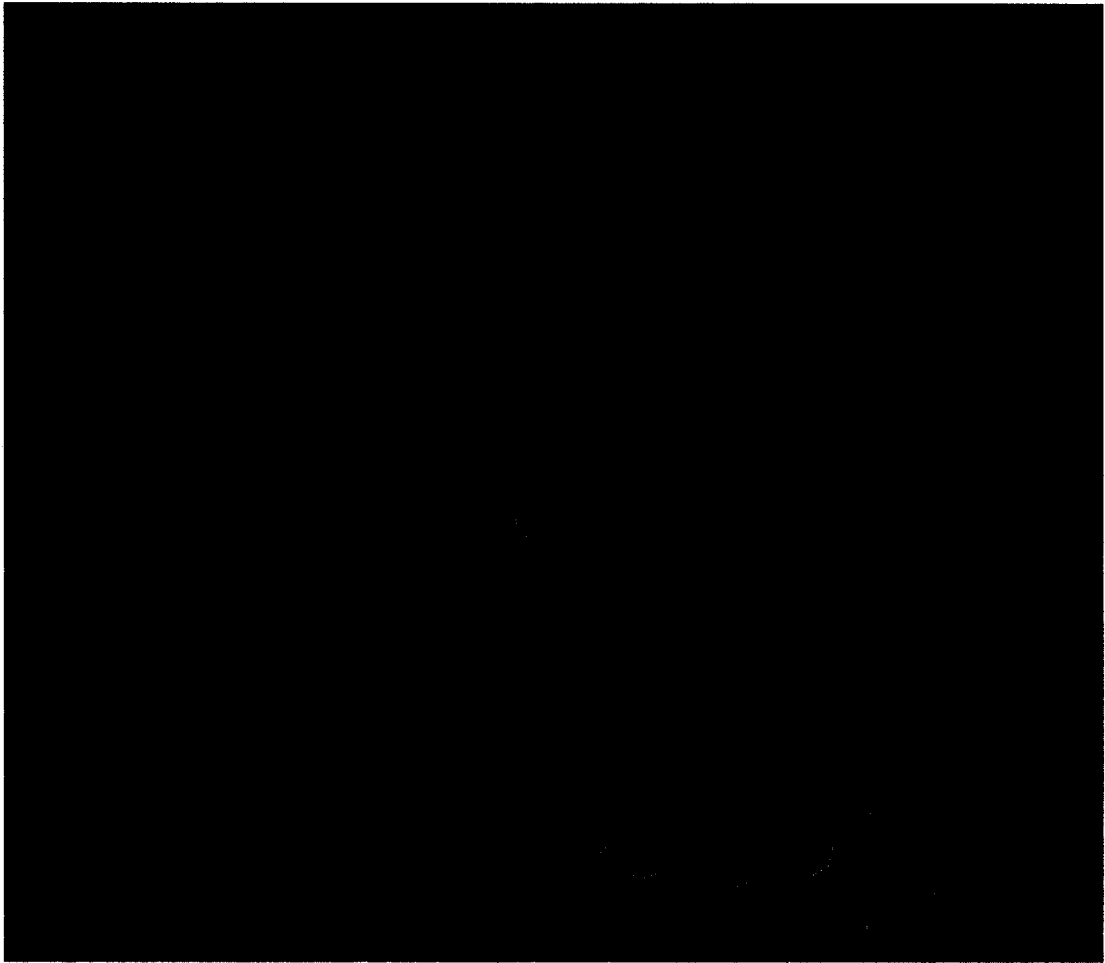
Figure 3

Figure 4

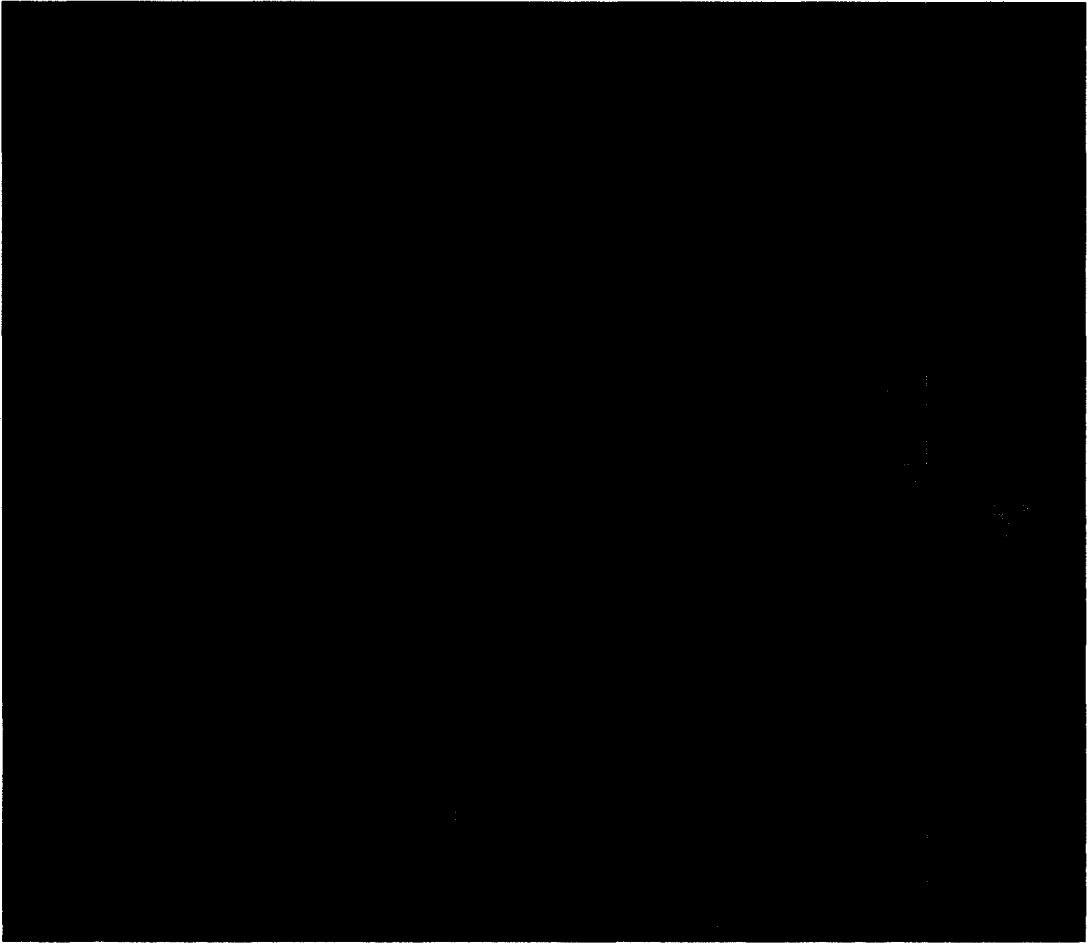Figure 5

Figure 6

Figure 7

Figure 8

CHAPTER 5 GENERAL CONCLUSIONS

An integrated system for protein crystallization screening at large scale in a high throughput manner was developed. The liquid handling subsystem has the capability of aspirating or dispensing 81 different or the same precipitants in a high throughput and parallel way. The volume range of solutions it can handle is between 20nL and 24uL. Small amount protein consumption as less as nanoliter for each condition significantly increases the total number of the conditions that can be screened. It also significantly reduces the time and efforts that cloning and protein expression require.

A new detection method, native fluorescence, which is highly compatible with high throughput and automatic protein crystallization screening, was introduced. The two detection schemes, the fluorescence and visible light methods, working together complementarily provide the system with the novel capability of distinguishing protein crystals from inorganic crystals in an automatic, non-destructive and high throughput manner, which no other method can achieve at this time. The whole system is cost effective. Each subsystem is especially designed and highly suitable for high throughput and automation. The crystallization of lysozyme was successfully demonstrated on this system.

A new crystallization method was developed. It is highly amenable to automation and high throughput protein crystallography because of its inherent properties. It significantly reduces the protein consumption by using nanoliter solutions. It further reduces the total protein consumption by exploring more space in a phase diagram for each single trial. It provides crystallographers one more parameter to take into control in crystallization screening experiments, the evaporation rate control. The protein crystals gotten by this method exhibits excellent diffraction quality. This method also has excellent scale up capability for growing large size crystals.

Human lactate dehydrogenase 1 (H4) complexed with NADH was successfully crystallized without adding any inhibitor and the best resolution of x-ray diffraction data is 2.5A. Heterogeneity in conformation of the active site loop has been observed among subunits in the same crystal and among multiple crystals. Existence of long-lived LDH conformers in solution is suggested.

ACKNOWLEDGEMENTS

I would like to take this opportunity to express my sincere appreciation to my mentor, Dr. Edward S. Yeung, who consistently spurs my interest in chemistry, teaches me how to find important problems and solve them creatively, and enlightens me with his unusual creativity, genuine interest in chemistry and consistent passion on science. He is also such a brilliant scientist whom I can always regard as my role model in my professional life. The research experience I gained and the methods for doing research I learnt in my Ph.D study under his guidance are invaluable treasure to me and will benefit my entire career forever.

I am very grateful to all my committee members, Dr. Donald C. Beitz, Dr. Robert S. Houk, Dr. Patricia A. Thiel, and Dr. Keith Woo for their precious time and advice. It is their kind supports that finally complete my Ph.D study.

I would also like to thank my collaborator, Dr. Howard Robinson at Brookhaven National Lab for his hard work and talent that made our collaboration very successful.

I greatly appreciate the endless support from the whole Dr. Yeung's group. I would like to thank Dr. Wei Wei, Dr. Yonghua Zhang, Dr. Hui Su, Dr. Xiaoyi Gong, Dr. Gang Xue, Dr. Hanlin Li , Dr. Wenwan Zhong, Dr. Jason Gruhaegen, Mr. Michael Christodoulou, Dr. Chanan Sluzny, Dr. Yan He, Dr. Jinjian Zheng and Dr. Zhiqiang Wang for their assistance to my research and the stimulating discussions, thank Aoshuang Xu, Hui Zhang, Guoxin Lu, Jiyoung Lee, Hung-Wing Li, Dragan Isailovic and Slavica Isailovic for their help, great friendship, and the wonderful time I spent with them. I am especially thankful to Dr. Wei Wei, Dr. Yonghua Zhang, Dr. Hui Su, for all the wonderful advice, continuously encouragement, and friendly support to my work and in my personal life.

At last, I want to thank all my family members especially my wife, Ella, for their consistent and endless support throughout my life.

APPENDIX 1

Our research work was chosen as a cover story.
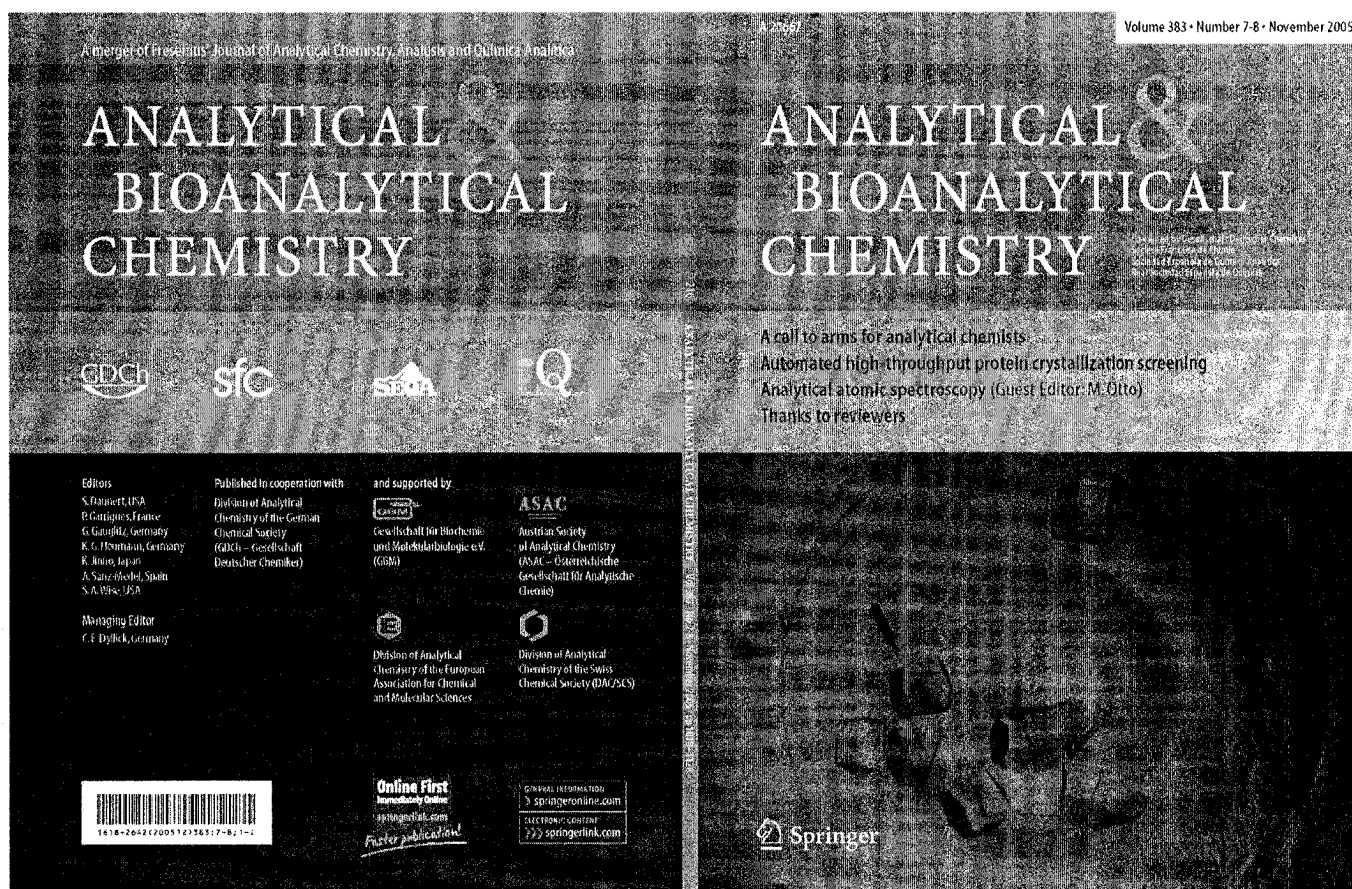
APPENDIX 2

Automated High Throughput Nanoliter-scale Protein Crystallization Screening

Edward S. Yeung and Fenglei Li

US11/283,138; US Patent Pending